Research Square

Preprints are preliminary reports that have not undergone peer review.
They should not be considered conclusive, used to inform clinical practice,
or referenced by the media as validated information.

Long-Term Spatio-Temporal Assessment of Land Use Dynamics and Ecosystem Service Values in Wadi Jazan, Saudi Arabia, Using GIS and Remote Sensing

Ibraheem A. H. Yousif
Cairo University
Abd Al-Rahman S. Ahmed
Cairo University
Wael Abdel-Moneim Omar
Taif University
Atef Fathy Ahmed
Taif University
A. E. Ibrahium
Aswan University
Fsaha Mebrahtu Gebru
fsahamebrahtu@rayu.edu.et
Raya University
Mohamed Metwally Mahmoud
Jadara University
Mohamed A. Atalla
Department of Natural Studies

Article

Keywords: Land use/land cover, Ecosystem service valuation, Spatio-temporal analysis, Wadi Jazan, Urban expansion, Value transfer, Sustainable land management, Climate adaptation

Posted Date: July 10th, 2026

DOI: https://doi.org/10.21203/rs.3.rs-10188861/v1

License: This work is licensed under a Creative Commons Attribution 4.0 International License. Read Full License

Additional Declarations: No competing interests reported.

Abstract

This study assessed spatio-temporal changes in land use/land cover (LULC) and ecosystem service values (ESVs) in Wadi Jazan, southwest Saudi Arabia, from 2000 to 2022. Using multi-temporal Landsat imagery, GIS, and a value transfer approach, six LULC classes were mapped and inter-decadal transitions analyzed. Results show a shift from agricultural expansion (2000–2011) to rapid urbanization (2011–2022), with built-up areas increasing nearly ninefold while agricultural land declined by ~ 18% and barren land was substantially converted in coastal plains and downstream wadi sections. Vegetation increased by ~ 12% in upland areas but remained fragmented in lowlands. Total ESV increased by ~ 7%, reflecting redistribution rather than ecological improvement, with strong trade-offs among ecosystem services and spatial inequality. Regulating services, including climate regulation, soil conservation, and biodiversity maintenance, declined by 10–25% in highly transformed zones. Water bodies exhibited the highest per-unit ESV, yet their area (< 5% of total) limited system-wide benefits. Spatial analysis identified degradation hotspots concentrated in coastal–fluvial zones, indicating high ecological vulnerability. The findings show that aggregate ESV gains can mask ecological degradation and highlight the need for spatially explicit assessment. Sustainable management requires watershed-scale ecosystem-based planning to balance development and ecological resilience under anthropogenic and climatic pressures.

1. Introduction

Coastal and fluvial ecosystems are among the most productive and ecologically significant systems worldwide, delivering a wide range of ecosystem services (ESs) that support human well-being, biodiversity conservation, climate regulation, and socio-economic development [1–3]. Functioning as dynamic interfaces between terrestrial, freshwater, and marine environments, these systems regulate hydrological processes, facilitate nutrient cycling, provide habitats for diverse species, and mitigate natural hazards such as floods and coastal erosion. In arid and semi-arid regions, where ecological resilience is inherently constrained by water scarcity and high climatic variability, the sustainability of coastal–fluvial ecosystems is particularly critical [4–6].

Wadi Jazan, located in southwest Saudi Arabia, represents a distinctive semi-arid coastal watershed characterized by strong interactions among upland catchments, agricultural landscapes, and the Red Sea coastal zone. The system provides a broad spectrum of ecosystem services, including provisioning services (e.g., freshwater supply, agriculture, and fisheries), regulating services (e.g., flood control, soil fertility maintenance, microclimate regulation, and coastal protection), supporting services (e.g., nutrient cycling and habitat provision), and cultural services related to recreation, aesthetics, and ecotourism [7–11]. These services are essential for sustaining local livelihoods and regional development, underscoring the ecological and socio-economic importance of Wadi Jazan. Over recent decades, however, Wadi Jazan has undergone substantial land use and land cover (LULC) changes driven by rapid urban expansion, agricultural intensification, infrastructure development, and industrial growth. Land-use changes in the region are closely linked to national development strategies, particularly Saudi Vision 2030, which promotes economic diversification, infrastructure expansion, and urban development. Regional initiatives aimed at agricultural development and water resource management have also influenced land-use patterns. However, limited integration of ecosystem service considerations into planning frameworks may contribute to observed ecological trade-offs between development and environmental sustainability. Strengthening policy alignment with ecosystem-based management principles is therefore essential.

Globally, LULC change is recognized as one of the most influential drivers of ecosystem service value (ESV) alteration and degradation [12–15]. In semi-arid environments, such transformations often result in vegetation loss, soil degradation, salinization, habitat fragmentation, and biodiversity decline, thereby reducing ecosystem capacity to deliver essential services [5, 16–20]. These pressures are further intensified by climate variability and growing anthropogenic demands, posing significant challenges for sustainable development in coastal watersheds.

Despite the growing application of ecosystem service valuation at global and regional scales, important knowledge gaps remain. Most existing studies emphasize humid or temperate regions, while semi-arid coastal–fluvial systems,

characterized by fragile ecosystems, rapid land transformation, and strong land–sea interactions, remain underrepresented [12, 13]. In Saudi Arabia, research has largely focused on urban ecosystems and mountainous watersheds (e.g., Riyadh, Jeddah, and Abha), with limited attention to integrated coastal–fluvial environments such as Wadi Jazan [21, 22]. Furthermore, many existing studies rely on static or short-term assessments, overlooking long-term spatio-temporal dynamics, cumulative anthropogenic impacts, spatial heterogeneity, and ecosystem service degradation hotspots [2, 8, 23–25]. In coastal regions, regulating services such as flood mitigation and coastal protection are often undervalued or overly generalized, limiting their usefulness for ecosystem-based planning and climate adaptation [26].

Recent advances in geographic information systems (GIS) and remote sensing (RS) have enabled robust, long-term, and spatially explicit assessments of LULC dynamics and ecosystem service values. Studies from rapidly transforming regions such as the Pearl River Delta, coastal Bangladesh, and Southeast Asia have documented significant declines in regulating and supporting services associated with urbanization and agricultural expansion, while also revealing complex trade-offs and synergies among ecosystem services [1, 2, 6, 26, 27]. Although recent geospatial studies in Saudi Arabia have reported ESV losses linked to urban growth and environmental stressors, semi-arid coastal watersheds such as Wadi Jazan remain comparatively underexplored despite their high ecological sensitivity and socio-economic importance [22, 28] .

Monetary valuation of ecosystem services provides a powerful decision-support tool by translating ecological change into economic terms that are directly relevant to policymakers and planners [1, 29]. Integrating multi-decadal remote sensing data with GIS-based ecosystem service valuation offers a comprehensive framework for assessing long-term spatio-temporal ESV dynamics, identifying degradation hotspots, and linking observed changes to specific land use drivers. This approach is particularly relevant for semi-arid coastal–fluvial systems, where competing land-use demands and climate stressors necessitate evidence-based, ecosystem-oriented management strategies.

This study addresses three key research gaps. First, semi-arid coastal–fluvial ecosystems such as Wadi Jazan remain underrepresented in ecosystem service assessments despite their high ecological sensitivity. Second, most existing studies rely on short-term or static analyses, limiting understanding of long-term spatio-temporal dynamics. Third, limited attention has been given to the spatial heterogeneity of ecosystem service degradation and hotspot identification in rapidly transforming dryland watersheds. By integrating multi-decadal remote sensing, GIS-based LULC analysis, and ecosystem service valuation, this study provides a spatially explicit and long-term assessment of ecosystem service dynamics. It advances current knowledge by linking land-use transitions to ecosystem service redistribution and identifying critical degradation hotspots to support sustainable land-use planning in semi-arid coastal–fluvial systems. This study contributes to the literature by providing one of the first long-term, spatially explicit assessments of ecosystem service dynamics in a semi-arid coastal–fluvial watershed, addressing a critical gap in dryland ecosystem research.

The present study conducts a long-term spatio-temporal assessment of ecosystem service value (ESV) changes in Wadi Jazan, southwest Saudi Arabia, by integrating multi-decadal LULC data with GIS and remote sensing techniques. The study aims to: (1) quantify land use and land cover changes in Wadi Jazan over the past two decades; (2) assess spatial and temporal variations in ecosystem service values in response to LULC dynamics; (3) identify key environmental and anthropogenic drivers influencing ESV changes; (4) delineate spatial hotspots of ecosystem service degradation and ecological vulnerability; and (5) provide science-based recommendations to support sustainable land-use planning, ecosystem conservation, and climate adaptation in semi-arid coastal–fluvial environments.

2. Materials and Methods

2.1. Study Area

The study was conducted in the Jazan region, located in southwestern Saudi Arabia along the eastern coast of the Red Sea (16°50'–17°30' N, 42°30'–43°30' E). The region covers approximately 256,757 ha and extends from low-lying coastal plains at sea level to mountainous terrain reaching elevations of up to 2,291 m (Fig. 1). This pronounced west–east topographic

gradient strongly controls local climate, vegetation distribution, hydrological processes, and overall ecosystem functioning [30–32]. The regional topography is illustrated by the digital elevation model (DEM) shown in Fig. 2.

The western Tihama coastal plain is characterized by sabkhas, mangroves, irrigated agricultural fields, and expanding urban settlements, whereas the eastern highlands and wadi systems support denser natural vegetation and fertile alluvial soils. This spatial heterogeneity underpins the provision of a wide range of ecosystem services, including provisioning (e.g., food and freshwater), regulating (e.g., climate regulation, water regulation, coastal protection), and supporting services related to soil fertility and biodiversity conservation [33–35]. Consequently, the region comprises diverse land use/land cover (LULC) classes—water bodies, croplands, natural vegetation, bare land, rocky outcrops, and built-up areas, making it well suited for spatially explicit ecosystem service value (ESV) assessments using remote sensing (RS) and geographic information system (GIS) techniques and the value transfer approach [36–38].

Climatically, the Jazan region experiences hot arid to semi-arid conditions. In 2024, the mean annual air temperature was approximately 31.3°C, with winter averages near 27.4°C and summer temperatures frequently exceeding 35.4°C in June. Maximum temperatures reached up to 42.6°C, while minimum temperatures remained relatively high throughout the year (22.5–30.9°C). Annual precipitation totaled about 495.7 mm, with rainfall concentrated in late summer, particularly in August (≈ 314 mm). Soil moisture and surface wetness followed this seasonal pattern, remaining low during dry months and peaking during the wet season. Relative humidity averaged 62.2% and increased during the rainy period due to Red Sea moisture influx, while wind speeds were generally moderate, with an annual mean of 3.24 m/s and stronger winds during summer months. Monthly climatic variations and their implications for LULC and ecosystem services are summarized in Fig. 3 and Table 1.

Rapid urban expansion, agricultural intensification, and infrastructure development over recent decades have substantially altered LULC patterns in the region, resulting in measurable changes in ecosystem service provision. The availability of multi-temporal satellite imagery and ancillary spatial data, combined with strong environmental gradients and anthropogenic pressures, makes the Jazan region an appropriate case study for assessing the impacts of land cover change on ecosystem services in arid and semi-arid coastal environments [39, 40].

Table 1
Monthly climatic parameters of the Jazan region for 2024 derived from NASA POWER data.

Parameter*	Jan	Feb	Mar	Apr	May	Jun	Jul	Aug	Sep	Oct	Nov	Dec	Annual Mean
SSW	0.27	0.23	0.21	0.22	0.18	0.16	0.21	0.49	0.47	0.34	0.32	0.27	0.28
P (mm d^{-1})	0.37	0.1	0.54	0.62	0.17	0.19	1.14	10.14	0.48	1.64	0.6	0.06	1.35
Psum or P (mm)	11.5	3.01	16.7	18.5	5.27	5.82	35.4	314.2	14.4	50.9	18.1	1.96	495.74
RH (%)	65.4	66.1	61.5	59.6	56.7	52.3	61.5	75.14	67.9	59.9	60.1	60.5	62.23
T (°C)	27.4	28	30.3	32.1	33.8	35.5	34.1	31.39	32.6	32.5	30.2	27.8	31.32
Tmax (°C)	31.2	31.9	35.5	37	38.5	42.6	39.3	35.48	38.8	39.6	35.5	32.2	42.57
Tmin (°C)	22.5	24.7	26.4	27.9	29.1	30.9	30.1	25.86	29.4	29.1	26.3	22.6	22.46
ΔT (°C)	4.94	4.97	5.17	5.56	5.96	6.59	6.09	4.3	4.87	5.18	5.23	5.63	5.37
WD_{10} (°)	240	244	220	214	258	255	279	279.9	258	263	234	211	250.2
WS_{10} (m s^{-1})	2.77	3.17	3.1	3.28	3.2	3.29	3.81	4.24	2.96	3.1	2.95	3.0	3.24
$WSmax_{10}$ (m s^{-1})	6.87	7.99	7.72	8.26	8.3	8.93	10.3	11.75	7.97	8.75	7.86	7.19	11.75
$WSmin_{10}$ (m s^{-1})	0.11	0.1	0.04	0.21	0.04	0.02	0.1	0.31	0.08	0.05	0.07	0.04	0.02
ΔWS_{10} (m s^{-1})	4.41	4.9	5.41	5.28	5.66	5.69	6.37	5.05	4.97	6.28	5.61	4.7	5.36

*SSW denotes surface soil wetness; P (mm d^{-1}) refers to daily precipitation; Psum or Ps (mm) represents cumulative precipitation; RH (%) refers to relative humidity; T (°C) is mean air temperature, while Tmax (°C) and Tmin (°C) denote maximum and minimum air temperatures, respectively; ΔT (°C) represents the temperature range. WD_{10} (°) denotes wind direction at 10 m height; WS_{10} (m s^{-1}) denotes mean wind speed at 10 m; $WSmax_{10}$ (m s^{-1}) and $WSmin_{10}$ (m s^{-1}) represent maximum and minimum wind speed at 10 m, respectively; ΔWS_{10} (m s^{-1}) denotes the wind speed range at 10 m.

2.2. Data sources

Multi-temporal satellite imagery was used to analyze LULC dynamics between 2000 and 2022. The year 2000 was selected as the baseline due to the availability and quality of consistent Landsat data, with subsequent observations at approximately 10-year intervals to capture long-term land cover changes. The selection of 2000, 2011, and 2022 reflects the availability of high-quality Landsat imagery and enables the representation of long-term decadal changes. However, the use of discrete time points may overlook short-term fluctuations and transitional dynamics.

Geometrically corrected Landsat Level 1 Terrain-corrected (L1T) products were obtained from the United States Geological Survey (USGS), including Landsat-5 TM (2000), Landsat-7 ETM+ (2011), and Landsat-8 OLI/TIRS (2022). All images were acquired during July to represent peak vegetation conditions while minimizing cloud contamination and were standardized to a spatial resolution of 30 m to ensure comparability.

Topographic information was derived from the Shuttle Radar Topography Mission (SRTM) 30 m digital elevation model (DEM), which was used to delineate the Wadi Jazan watershed and extract elevation, slope, flow accumulation, and drainage networks. These variables supported the interpretation of hydrological patterns and LULC distribution across the study area [41, 42]. All datasets were subjected to standard preprocessing procedures, including radiometric and atmospheric

corrections, and spatial subsetting to the study area. A summary of the Landsat datasets used is provided in Table 2, while the overall methodological framework is illustrated in Fig. 4.

Table 2
Summary of Landsat satellite datasets used for multi-temporal land use/land cover (LULC).

Landsat Sensor	Path/Row	ID of imagery	Resolution (m)
Landsat 5 TM	164/41	LT05_L1TP_167048_20000731_20200906_02_T1	30
Landsat 7 ETM+	164/41	LE07_L1TP_167048_20110823_20200909_02_T1	30
Landsat 9 OLI&TIRS	164/41	LC09_L1TP_167048_20220704_20230408_02_T1	30

2.3. Image pre-processing and LULC classification

The methodological workflow integrates remote sensing (RS), GIS, and ecosystem service valuation techniques to quantify spatio-temporal changes in LULC and their impacts on ESVs (Fig. 4). All Landsat images were preprocessed in ArcGIS 10.5, starting with radiometric calibration to convert digital numbers to top-of-atmosphere reflectance, followed by atmospheric correction to minimize atmospheric absorption and scattering effects [43–45]. These procedures ensured consistency across sensors and acquisition dates while reducing uncertainties in subsequent analyses.

Supervised classification was applied to the processed imagery using the Maximum Likelihood classifier, with spectral signatures supported by ancillary data, visual interpretation, and field knowledge. While advanced machine-learning approaches such as Random Forest and Support Vector Machines may enhance classification performance, the Maximum Likelihood method remains a reliable and widely used approach for multi-temporal Landsat analysis. Its suitability is supported by the relatively high classification accuracies (81–87%) achieved in this study. Nevertheless, some confusion persisted among spectrally similar classes, particularly bare land, rocky surfaces, and built-up areas, representing a recognized limitation. Post-classification refinement techniques were further applied to reduce misclassification and improve thematic accuracy [46, 47].

Based on regional characteristics and consistency with previous ecosystem service studies, six major LULC classes were identified: water bodies, cultivated land, natural vegetation, built-up areas, bare land, and rocky outcrops (Table 3). Although this generalized classification scheme may simplify landscape heterogeneity and mask finer ecological distinctions, especially within vegetation and urban categories, it was adopted to ensure compatibility with Landsat spatial resolution and comparability with existing ecosystem service valuation studies. The classified LULC maps formed the basis for subsequent change detection and ESV estimation, enabling the assessment of spatial patterns, temporal trends, and land cover-driven ecosystem service dynamics [7, 28, 48].

Table 3
Classification scheme and description of major land use/land cover (LULC) categories identified in the Wadi Jazan study area.

Land Cover Types	Description
Water Bodies	Surface water features include rivers, lakes, reservoirs, and coastal or inland water bodies.
Cultivated Areas	Agricultural lands used for crop production, including irrigated and rain-fed fields.
Natural Vegetation	Naturally occurring vegetation such as grasslands, shrubs, and sparse desert vegetation.
Built-up Areas	Urban, industrial, residential, and infrastructural areas dominated by impervious surfaces.
Bare Land	Exposed soil surfaces with little or no vegetation cover, including barren and degraded lands.
Rock Land (Rocky Outcrops)	Areas dominated by exposed bedrock or rocky surfaces with negligible soil development.

2.4. Accuracy assessment

Classification accuracy was evaluated using standard accuracy assessment procedures. Reference data were obtained from high-resolution imagery (Google Earth Pro), field observations, and existing thematic maps [44, 49]. Stratified random sampling points were generated for each LULC class and compared with reference data to construct error matrices.

Overall accuracy (OA) and the kappa coefficient (κ) were calculated to quantify agreement between classified maps and ground truth data. The kappa coefficient was computed as:

$$kappa\ coefficient = \frac{\sum_{i=1}^{m} X_{ii} - \sum_{i=1}^{m} X_{ii}\,(A_i C_i)}{n^2 - \sum_{i=1}^{m} X_{ii}\,(A_i C_i)}$$

where *n* is the total number of stratified random samples taken, X_{ii} gives the number of samples in actual class i, A_i is the total number of actual ground truth samples associated with class i C_i represents the total number of the classified sample belonging to class i, *m* is numbers of rows and columns in the error matrix. The kappa coefficient ranges from − 1 to + 1, with higher values indicating stronger agreement; values greater than 0.80 represent excellent agreement, 0.60–0.80 indicate substantial agreement, and values below 0.60 suggest moderate to low agreement [43, 49, 50].

In addition, producer's accuracy (PA) and user's accuracy (UA) were calculated to evaluate errors of omission and commission for individual LULC classes [46, 51]. This multi-source validation approach ensures that the classified LULC maps accurately represent real-world conditions and provide a reliable foundation for subsequent ecosystem service value (ESV) assessments.

It is important to note that classification uncertainty may propagate into subsequent ecosystem service value (ESV) estimates, as valuation is directly dependent on mapped land-cover areas. Misclassification among spectrally similar classes, particularly built-up areas, bare land, and rocky surfaces, may therefore introduce uncertainty into ESV calculations. This limitation is acknowledged and considered in the interpretation of results.

2.5. LULC change detection (2000–2022)

LULC changes between 2000 and 2022 were quantified using a post-classification comparison approach implemented in ArcGIS Pro. Classified LULC maps for each year were overlaid using raster analysis tools to identify transitions among land cover classes. Transition matrices were generated using the Raster Calculator and Tabulate Area tools, allowing quantification of both the area and percentage of land converted from one class to another. This approach enabled the identification of dominant trends, including urban expansion, changes in cultivated land, vegetation loss or recovery, and

variations in water bodies and bare land. Post-classification comparison is particularly effective for multi-temporal studies because it minimizes the influence of sensor differences and atmospheric variability [50, 52, 53].

2.6. Ecosystem service value assessment

Ecosystem service values were estimated using the value transfer approach, which applies standardized monetary coefficients to spatially explicit LULC data. Baseline ESV coefficients were derived primarily from Costanza, d'Arge, De Groot, Farber, Grasso, Hannon, Limburg, Naeem, O'neill and Paruelo [36]; Costanza, De Groot, Sutton, Van der Ploeg, Anderson, Kubiszewski, Farber and Turner [37] and De Groot, Brander, Van Der Ploeg, Costanza, Bernard, Braat, Christie, Crossman, Ghermandi and Hein [38], supplemented by the Ecosystem Services Valuation Database (ESVD) and regionally relevant studies to better reflect semi-arid coastal conditions [22, 54, 55].

Each LULC class was assigned a representative ESV coefficient expressed in USD/ha/year (Table 4). Water bodies were assigned the highest value (12,512 USD/ha/year) due to their critical roles in hydrological regulation, water purification, and habitat provision. Cultivated land was valued at 5,567 USD/ha/year, reflecting food production and supporting services. Natural vegetation was assigned values ranging from 3,800 to 4,166 USD/ha/year to represent regulating and supporting functions such as carbon sequestration, soil stabilization, and biodiversity conservation. Built-up areas were assigned a value of 6,661 USD/ha/year to capture economic contributions, while bare land and rocky outcrops were assigned zero value due to their limited measurable ecosystem services in semi-arid environments. The total ESV for each LULC category was calculated using the standard formula:

$$ESV = \sum \left(A_{\mathrm{i}} \times \ \mathrm{VC}_i\right)$$

where ESV is the total ecosystem service value of each land type, A_{i} represents the area of land cover type in hectares, and VC_i denotes the corresponding ESV coefficient in USD/ha/year. Multiplying the coefficient by the area provides a spatially explicit estimate of ecosystem services across the study area, enabling the identification of high-value ecological zones and informing sustainable land management and policy strategies. The relatively high coefficient assigned to built-up areas reflects aggregated economic and cultural services derived from urban systems as reported in global valuation frameworks. However, this value does not represent ecological service provision and may overestimate ecosystem functionality in urban landscapes. Therefore, urban ESV values should be interpreted cautiously and primarily as indicators of socio-economic contributions rather than ecological benefits.

The value transfer method is widely applied in ecosystem service assessments where site-specific valuation data are unavailable and has been successfully used across diverse landscapes, including arid, coastal, and urban environments [1, 49, 53]. Although uncertainties remain, sensitivity analyses and transparent discussion of limitations support its use for informing sustainable land management and policy decisions in the Jazan region.

A sensitivity analysis was conducted by adjusting ESV coefficients by ± 25% and ± 50% to assess the robustness of valuation results and quantify uncertainty associated with the benefit transfer approach. This analysis provides insight into how variations in coefficient values influence total ESV estimates and supports the reliability of comparative trend analysis despite inherent uncertainties.

Table 4
Economic Services Value (ESV) coefficients for different Land Use/Land Cover (LULC) categories in Jazan valley, expressed in USD/ha/year.

LULC Class	Biome Equivalent (Costanza)	ESV (USD/ha/yr)	Rationale and justification
Water	Lakes and river	12,512	Provides key hydrological, regulatory, and habitat-supporting services. Adopted from global valuation by Costanza, d'Arge, De Groot, Farber, Grasso, Hannon, Limburg, Naeem, O'neill and Paruelo [36] as a benchmark for high-value aquatic ecosystems.
Cultivated Areas	Cropland	5,567	Represents provisioning services, including food production and supporting ecosystem functions. Values derived via benefit transfer from Costanza, d'Arge, De Groot, Farber, Grasso, Hannon, Limburg, Naeem, O'neill and Paruelo [36] and regional adjustments [54].
Natural Vegetation	Forest Grassland	3,800–4,166	Captures regulating and supporting services such as climate moderation, soil stabilization, and biodiversity conservation. Values based on Costanza, d'Arge, De Groot, Farber, Grasso, Hannon, Limburg, Naeem, O'neill and Paruelo [36] and Costanza, De Groot, Sutton, Van der Ploeg, Anderson, Kubiszewski, Farber and Turner [37] and adjusted for vegetation density and regional context [54].
Built-Up Areas	Urban	6,661	Reflects primarily direct economic contributions of urban areas while acknowledging limited provision of natural ecosystem services [36, 37].
Bare Land	Barren land	0	Typically contributes negligible measurable ecosystem services; zero value is used for dryland and semi-arid contexts [36, 37].
Rock Land	Rock	0	Similar to bare land; minimal or no ecosystem service provision [36, 37].

3. Results

3.1. Accuracy assessment and reliability of LULC classification

The supervised classification of multi-temporal Landsat imagery for 2000, 2011, and 2022 generated internally consistent and statistically robust LULC maps (Fig. 5). The detailed confusion matrices and accuracy metrics are presented in Table 5, including overall accuracy, Kappa coefficient, and class-specific user's and producer's accuracies. Overall classification accuracies exceeded the commonly accepted 80% threshold for land change studies in all years, confirming the suitability of the dataset for subsequent spatial and ecosystem service analyses.

For the year 2000, the overall accuracy reached 81%, with a Kappa coefficient of 0.71, indicating substantial agreement between classified outputs and reference data. Water achieved perfect user and producer accuracies (1.00), reflecting its distinct spectral signature and spatial coherence. Natural vegetation also demonstrated high classification performance (user accuracy = 0.89; producer accuracy = 0.67). In contrast, built-up areas recorded the lowest user accuracy (0.20), primarily due to spectral confusion with bare land and rock land in sparsely developed zones. Bare land showed moderate performance (producer accuracy = 0.58), reflecting mixed pixels and transitional surfaces typical of semi-arid environments.

In 2011, classification reliability improved slightly, with overall accuracy increasing to 82% and a Kappa value of 0.73. Water and rock land maintained high user accuracies (1.00 and 0.94, respectively), while natural vegetation exhibited strong performance (user accuracy = 0.91; producer accuracy = 0.84). However, bare land showed a relatively low producer accuracy (0.43), indicating greater confusion with cultivated and built-up areas during this period of intensified agricultural expansion.

By 2022, classification performance further improved, reaching an overall accuracy of 87% and a Kappa coefficient of 0.83, reflecting near-excellent agreement. Water maintained perfect accuracy (user and producer accuracy = 1.00), while cultivated land demonstrated strong discrimination (user accuracy = 0.80; producer accuracy = 0.88). Built-up areas

exhibited notable improvement (user accuracy = 0.60; producer accuracy = 0.75), likely attributable to enhanced spatial resolution, refined training datasets, and clearer urban spectral signatures associated with rapid infrastructure expansion. Collectively, the results in Table 5 confirm that the adopted classification methodology reliably captured the spatio-temporal dynamics of land use and land cover across the 22-year study period.

Table 5

Quantitative analysis and accuracy assessment of LULC classification for 2000, 2011, and 2022 in the Jazan Valley, highlighting land transformation trends and sub-period variations.

Year			Referenced Data							
		Class	Water	Cultivated Land	Bare Land	Built Up	Natural Vegetation	Rock Land	Total	User Accuracy
2000	Classified Data	Water	10.00	0.00	0.00	0.00	0.00	0.00	10.00	1.00
		Cultivated Land	0.00	4.00	2.00	0.00	0.00	1.00	7.00	0.57
		Bare Land	0.00	0.00	11.00	0.00	0.00	3.00	14.00	0.79
		Built Up	0.00	0.00	4.00	1.00	0.00	0.00	5.00	0.20
		Natural Vegetation	0.00	0.00	0.00	0.00	8.00	1.00	9.00	0.89
		Rock Land	0.00	2.00	2.00	0.00	4.00	47.00	55.00	0.85
		Total	10.00	6.00	19.00	1.00	12.00	52.00	100.00	0.00
		P Accuracy	1.00	0.67	0.58	1.00	0.67	0.90	0.00	0.81
		Overall Accuracy	0.81			Kappa = 0.71				
2011	Classified Data	Water	10	0.0	0.0	0.0	0.0	0.0	10	1.0
		Cultivated Land	0.0	5.0	2.0	0.0	0.0	2.0	9.0	0.55
		Bare Land	0.0	0.0	7.0	0.0	0.0	3.0	10.0	0.7
		Built Up	0.0	0.0	7.0	2	0.0	0.0	9.0	0.22
		Natural Vegetation	1.0	0.0	0.0	0.0	11.0	0.0	12.0	0.91
		Rock Land	0.0	1.0	0.0	0.0	2.0	47.0	50.0	0.94
		Total	11	6.0	16	2.0	13.0	52.0	100.0	0.0
		P Accuracy	0.90	0.83	0.43	1.0	0.84	0.90	0.0	0.82
		Overall Accuracy	0.82			Kappa = 0.73				
2022	Classified Data	Water	10.0	0.0	0.0	0.0	0.0	0.0	10.0	1.0
		Cultivated Land	0.0	8.0	1.0	0.0	0.0	1.0	10.0	0.8
		Bare Land	0.0	1.0	9.0	0.0	0.0	0.0	9.0	1.0
		Built Up	0.0	0.0	3.0	6.0	0.0	0.0	10.0	0.6
		Natural Vegetation	0.0	0.0	0.0	1.0	10.0	1.0	12.0	0.83
		Rock Land	0.0	0.0	3.0	1.0	0.0	44.0	48.0	0.91
		Total	10.0	9.0	16	8.0	10.0	46.0	99.0	0.0

P Accuracy	1.0	0.88	0.56	0.75	1.0	0.95	0.0	0.87
Overall Accuracy	0.87			Kappa = 0.83				

3.2. Spatial distribution and composition of LULC classes

The spatial distribution of LULC classes across the watershed demonstrates strong geomorphological and hydrological controls (Fig. 5). The LULC transition matrix (Table 6) confirms that natural vegetation and bare land were the primary sources for both cultivated and built-up land expansion across both periods, highlighting a consistent pattern of terrestrial ecosystem conversion. The total study area remained constant at 256,759 ha for all three reference years, ensuring consistent inter-temporal comparison. Six primary LULC classes were identified: water, cultivated areas, natural vegetation, built-up areas, bare land, and rock land. Rock land consistently dominated the landscape, reflecting the rugged geomorphological structure of the watershed and extensive exposure of bedrock in upland areas. Its areal extent decreased from 180,361 ha (70.25%) in 2000 to 161,345 ha (62.84%) in 2011, before partially recovering to 169,994 ha (66.21%) in 2022. This fluctuation indicates localized land conversion during the initial phase of agricultural expansion and infrastructure development, followed by partial stabilization in the later period.

Table 6
LULC transition matrix for 2000, 2011, and 2022 in the Jazan Valley, highlighting the role of natural vegetation and bare land in cultivated and built-up land expansion.

LULC	**Landsat 5 TM 2000**		**Landsat 7 ETM 2011**		**Landsat 8 OLI and TIR 2022**	
	***ha**	****%**	**ha**	**%**	**ha**	**%**
Water	219.00	0.09	473.00	0.18	418.00	0.16
Cultivated Areas	8,503.00	3.31	25,896.00	10.09	9,079.00	3.54
Natural Vegetation	27,394.00	10.67	39,218.00	15.27	49,538.00	19.29
Built Up Areas	1,570.00	0.61	2,592.00	1.01	14,269.00	5.56
Bare Land	38,712.00	15.08	27,235.00	10.61	13,461.00	5.24
Rock Land	180,361.00	70.25	161,345.00	62.84	169,994.00	66.21
Total	256,759.00	100.00	256,759.00	100.00	256,759.00	100.00

*Hectare (ha = 10000 m^2).

** Expansion percentage.

Bare land exhibited a continuous and pronounced decline over the study period, decreasing from 38,712 ha (15.08%) in 2000 to 27,235 ha (10.61%) in 2011 and further to 13,461 ha (5.24%) in 2022. This downward trend reflects progressive transformation of previously undeveloped surfaces into cultivated, vegetated, or urban land, facilitated by irrigation development and land reclamation projects. Natural vegetation displayed a steady and substantial increase, expanding from 27,394 ha (10.67%) in 2000 to 39,218 ha (15.27%) in 2011 and reaching 49,538 ha (19.29%) in 2022. This sustained growth suggests improved water management practices, episodic rainfall variability, vegetation recovery along wadi corridors, and expansion along irrigated agricultural margins. Cultivated areas experienced contrasting trends between the two sub-periods. From 2000 to 2011, cultivated land expanded dramatically from 8,503 ha (3.31%) to 25,896 ha (10.09%), representing the most significant proportional increase among all classes during this phase. However, by 2022, cultivated land declined sharply to 9,079 ha (3.54%), reflecting reallocation of agricultural land to urban uses, water scarcity constraints, soil salinization, and shifting socio-economic priorities. The most striking transformation occurred in built-up areas, which increased from 1,570 ha (0.61%) in 2000 to 2,592 ha (1.01%) in 2011 and surged to 14,269 ha (5.56%) in 2022.

This more than nine-fold expansion highlights rapid urbanization, infrastructure development, and population growth, particularly after 2011. Water bodies remained limited in spatial extent, fluctuating slightly from 219 ha (0.09%) in 2000 to 473 ha (0.18%) in 2011 and 418 ha (0.16%) in 2022, reflecting hydrological variability rather than permanent expansion.

3.3. Spatio-temporal land cover change (2000–2022)

Changes from 2000 to 2022, as well as net changes across sub-periods, are summarized in Table 7. The trends in land cover change for 2000, 2011, and 2022 are presented in Fig. 6. Land use/land cover (LULC) patterns in Jazan Valley from 2000 to 2022 demonstrate substantial spatial reorganization driven by agricultural expansion, rapid urbanization, and environmental variability. Rock land consistently dominated the landscape, accounting for 180,361 ha (70.25%) in 2000, decreasing to 161,345 ha (62.84%) in 2011, and partially recovering to 169,994 ha (66.21%) in 2022. This trajectory reflects an initial phase of intensive land conversion, primarily for agriculture and infrastructure, followed by a relative reduction in conversion pressure and increased geomorphological exposure in the later period. Bare land declined steadily and markedly from 38,712 ha (15.08%) in 2000 to 27,235 ha (10.61%) in 2011 and further to 13,461 ha (5.24%) in 2022. This continuous reduction indicates progressive land transformation, largely driven by conversion to cultivated land, natural vegetation, and urban areas, supported by irrigation expansion and land development initiatives. Natural vegetation exhibited sustained and significant growth, increasing from 27,394 ha (10.67%) in 2000 to 39,218 ha (15.27%) in 2011 and reaching 49,538 ha (19.29%) in 2022. This trend suggests improved water availability, expansion of irrigated zones, and ecological regeneration along wadi systems and floodplains. Cultivated areas showed pronounced temporal variability. They expanded sharply from 8,503 ha (3.31%) in 2000 to 25,896 ha (10.09%) in 2011, reflecting a period of strong agricultural intensification. However, by 2022, cultivated land declined significantly to 9,079 ha (3.54%), indicating a contraction likely associated with urban encroachment and shifting land-use priorities. Built-up areas recorded the most dramatic increase over the study period, rising from 1,570 ha (0.61%) in 2000 to 2,592 ha (1.01%) in 2011, and then surging to 14,269 ha (5.56%) in 2022. This rapid expansion highlights the acceleration of urban growth, particularly during the 2011–2022 period. Water bodies remained a minor but relatively stable component, increasing from 219 ha (0.09%) in 2000 to 473 ha (0.18%) in 2011, followed by a slight decline to 418 ha (0.16%) in 2022, indicating limited hydrological fluctuation.

LULC dynamics in Jazan Valley from 2000 to 2022 indicates significant geographical and temporal changes influenced by agricultural expansion, swift urban development, and environmental fluctuations. The LULC dynamics reveal a two-phase trajectory: an initial period (2000–2011) dominated by agricultural expansion and vegetation growth, followed by a second phase (2011–2022) characterized by rapid urbanization, contraction of cultivated land, and continued ecological expansion.

Table 7
Land use/land cover (LULC) patterns in Jazan Valley from 2000 to 2022.

LULC	2000		2011		2022	
	*ha	**%	ha	%	ha	%
Water	219.00	0.09	473.00	0.18	418.00	0.16
Cultivated Areas	8,503.00	3.31	25,896.00	10.09	9,079.00	3.54
Natural Vegetation	27,394.00	10.67	39,218.00	15.27	49,538.00	19.29
Built Up Areas	1,570.00	0.61	2,592.00	1.01	14,269.00	5.56
Bare Land	38,712.00	15.08	27,235.00	10.61	13,461.00	5.24
Rock Land	180,361.00	70.25	161,345.00	62.84	169,994.00	66.21
Total	256,759	100	256,759.	100	256,759	100

*Hectare (ha = 10000 m^2).

** Proportion of each LULC class relative to the total study area.

Figure 6 shows marked changes in land cover composition, notably the expansion of built-up areas from 1,570 ha in 2000 to 14,269 ha in 2022, largely at the expense of vacant and agricultural land, particularly after 2011. Natural vegetation increased steadily, while cultivated land peaked in 2011 and declined significantly by 2022, reflecting shifting land-use priorities. The Jazan Valley transitioned from agriculture-driven growth (2000–2011) to rapid urban expansion and landscape reconfiguration (2011–2022). Although increased vegetation may enhance ecosystem services, concentrated urban growth poses trade-offs between development and environmental sustainability, highlighting the need for integrated land-use planning and sustainable water management in arid and semi-arid regions.

3.4. Land use/land cover transition matrix (2000–2022)

The land use/land cover (LULC) transition matrix for 2000–2022 (Table 8) provides quantitative evidence of substantial landscape reorganization across Wadi Jazan, southwestern Saudi Arabia. The observed transition patterns reveal a spatially heterogeneous system shaped by the interaction of geomorphological constraints, hydrological dynamics, and development-driven land-use change. Distinct contrasts are evident between the upper catchment, middle wadi reaches, and coastal plain, reflecting environmental gradients and recent development trajectories associated with regional growth strategies.

Analysis of the diagonal elements in Table 8 indicates strong persistence in geomorphologically constrained classes. Rock land exhibits the highest stability, with 146,062.30 ha remaining unchanged over the 22-year period. This persistence reflects the dominance of exposed bedrock, steep slopes, and rugged terrain in upland and peripheral zones, where land conversion is limited by topography, lithology, and accessibility. Bare land also shows considerable stability (9,714.49 ha), consistent with widespread arid surface conditions and low land-use intensity along wadi margins. Natural vegetation retained 18,794.54 ha, indicating moderate persistence within ecologically suitable zones. Water bodies experienced minimal spatial change, reflecting the ephemeral hydrological regime characterized by seasonal rainfall and short-lived runoff rather than permanent storage.

In contrast, off-diagonal elements of Table 8 demonstrate strong anthropogenic influence, particularly in the middle and lower reaches of the basin. Built-up areas expanded markedly, primarily through the conversion of bare land (6,810.68 ha) and cultivated land (3,048.46 ha). These transitions indicate urban encroachment into previously agricultural and undeveloped areas and are spatially concentrated along the Wadi Jazan corridor and near established urban centers, where favorable terrain and expanding infrastructure facilitated development. Cultivated land experienced substantial contraction, with only approximately 1,796 ha remaining unchanged. Significant portions were converted to built-up areas, bare land (~ 991 ha), and rock land (1,814 ha), reflecting a combination of urban expansion and declining agricultural viability. Factors such as water scarcity, soil salinization, and competition for groundwater likely contributed to reduced sustainability in marginal farmlands. Bare land functioned as a dynamic transitional class within the LULC system. Beyond its internal persistence, it was extensively converted to cultivated land (6,406.48 ha) and built-up areas (6,810.68 ha), highlighting its role as a spatial reserve for agricultural expansion and urban growth. Conversely, substantial conversion from bare land to rock land (14,876.17 ha) suggests surface erosion, sediment stripping during episodic flood events, and enhanced exposure of lithological surfaces. Improved sensor resolution and classification performance may also have enhanced the detection of exposed bedrock in later imagery. Natural vegetation exhibited bidirectional transitions. Conversions from natural vegetation to rock land (7,506.42 ha) suggest localized degradation driven by grazing pressure, resource extraction, and climatic stress. Conversely, the transition from rock land to natural vegetation (29,207.28 ha) indicates vegetation recovery in specific zones, potentially associated with favorable rainfall, moisture retention in fractured substrates, and reduced anthropogenic disturbance in remote upland areas.

The LULC transition matrix (Table 8) demonstrates increasing landscape reorganization driven by human activity in the middle and lower reaches of Wadi Jazan, where urban expansion and agricultural decline are most pronounced. In contrast, upper catchment areas remain largely controlled by geomorphological factors. These results underscore the need for spatially differentiated land-use planning that supports sustainable urban development in the coastal plain, safeguards

productive agricultural land along the wadi floor, and conserves ecological functions in upstream arid and semi-arid environments.

Table 8
Quantitative Land Use/Land Cover (LULC) Transition Matrix Showing Class Persistence and Inter-Class Conversion Pathways in Jazan Valley from 2000 to 2022 (Area in Hectares).

LULC 2000\ LULC 2022	Water	Built-up	Cultivated Areas	Bare Land	Rock Land	Natural Vegetation	Total (ha)
Water	191.13	0.00	0.00	0.00	11.47	16.50	219.10
Built-up Areas	0.00	839.24	57.14	68.85	520.56	4.89	1,490.68
Cultivated Areas	15.27	3,048.46	1,796.42	991.48	1,813.51	624.55	8,289.69
Bare Land	42.75	6,810.68	6,406.48	9,714.49	14,876.17	290.68	38,141.25
Rock Land	127.10	3,387.77	634.53	2,443.16	146,062.30	29,207.28	181,861.14
Natural Vegetation	42.51	82.90	138.03	94.74	7,506.42	18,794.54	26,658.14
Total (2022)	418.76	14,169.05	9,032.61	13,412.72	170,290.43	48,938.44	256,660.00

Figure 7 illustrates spatially heterogeneous LULC transitions shaped by geomorphology, hydrology, and development-driven land-use change. Clear contrasts appear among the upper catchment, middle wadi reaches, and coastal plain, reflecting environmental gradients and recent development aligned with Saudi Vision 2030. Transitions are concentrated along Wadi Jazan and adjacent to existing urban areas, where favorable topography and expanding infrastructure have accelerated urban growth, underscoring Wadi Jazan's growing role as a regional economic hub.

3.5. Evaluation of alterations in ecosystem service value (ESV)

The assessment of Ecosystem Service Value (ESV) in Wadi Jazan reveals pronounced temporal changes in both magnitude and composition between 2000 and 2022. Total ESV increased from 170.1 million USD/year in 2000 to 324.26 million USD/year in 2011, and further to 348.89 million USD/year in 2022 (Table 9). In 2000, Natural Vegetation dominated ecosystem services (109.58 million USD; 64.44%), followed by Cultivated Areas (47.34 million USD; 27.83%). Built-Up Areas (10.45 million USD; 6.14%) and Water (2.74 million USD; 1.61%) contributed marginally, while Bare Land and Rock Land had negligible ESV (Table 9). By 2011, total ESV more than doubled. Cultivated Areas (144.21 million USD; 44.45%) nearly equaled Natural Vegetation (156.87 million USD; 48.37%), reflecting agricultural expansion. Built-Up Areas remained limited (5.32%). In 2022, total ESV rose moderately, but its structure shifted significantly. Natural Vegetation regained prominence (198.15 million USD; 56.81%), while Built-Up Areas increased sharply to 95 million USD (27.21%), indicating accelerated urban expansion. Cultivated Areas declined markedly to 50.51 million USD (14.48%), and Water slightly decreased (5.23 million USD; 1.50%) (Table 9). Spatial patterns of ESV distribution demonstrate clear heterogeneity across the watershed, with higher values concentrated in vegetated and agricultural zones and lower values in built-up and barren areas (Fig. 8).

Table 9
Ecosystem Service Value (ESV) estimated in Million United State Dollars per year (M. USD/Yr) and percentage (%) contribution by LULC class in Wadi Jazan for the years of 2000, 2011, and 2022.

LULC Class	ESV (2000)		ESV (2011)		ESV (2022)	
	M. USD/Yr	%	M. USD/Yr	%	M. USD/Yr	%
Water	2.74	1.61	5.91	1.82	5.23	1.5
Cultivated Areas	47.34	27.83	144.21	44.45	50.51	14.48
Natural Vegetation	109.58	64.44	156.87	48.37	198.15	56.81
Built-Up Areas	10.45	6.14	17.26	5.32	95	27.21
Bare Land	0	0	0	0	0	0
Rock Land	0	0	0	0	0	0
Total	170.1	100	324.26	100	348.89	100

3.6. Changes in ESV (ΔESV) and land use transitions

Changes in ESV (ΔESV) across 2000–2011, 2011–2022, and 2000–2022 are summarized in Table 10. Between 2000 and 2011, Cultivated Areas recorded the largest increase (+ 96.87 million USD; +204.7%), followed by Natural Vegetation (+ 47.29 million USD; +43.2%). Water and Built-Up Areas showed moderate gains, while Bare and Rock Land remained unchanged. From 2011 to 2022, Built-Up Areas exhibited the most substantial increase (+ 77.74 million USD; +450.3%), reflecting rapid urbanization. In contrast, Cultivated Areas declined sharply (− 93.7 million USD; −65%), indicating conversion to urban uses or land abandonment. Natural Vegetation continued to grow (+ 41.28 million USD; +26.3%), while Water experienced a slight decline (− 0.68 million USD; −11.5%). Over the full study period (2000–2022), total ESV increased by 178.79 million USD (+ 105.1%), primarily driven by expansion in Built-Up Areas and Natural Vegetation (Table 10). However, this growth reflects structural redistribution rather than uniform ecological improvement.

Table 10
Change (%) in ecosystem service value (ΔESV) by LULC class for the periods 2000–2011, 2011–2022, and 2000–2022.

LULC Class	2000–2011		2011–2022		2000–2022	
	ΔESV	%	ΔESV	%	ΔESV	%
Water	3.17	115.7	-0.68	-11.5	2.49	90.9
Cultivated Areas	96.87	204.7	-93.7	-65	3.17	6.7
Natural Vegetation	47.29	43.2	41.28	26.3	88.57	80.8
Built-Up Areas	6.81	65.2	77.74	450.3	84.55	809.7
Bare Land	0	0	0	0	0	0
Rock Land	0	0	0	0	0	0
Total	154.16	90.6	24.63	7.6	178.79	105.1

Integration with the LULC transition matrix (Table 11) highlights major transfer pathways. Cultivated land was converted to Built-Up Areas and Bare Land, while Bare and Rock Lands significantly contributed to urban expansion. Conversely, large portions of Rock Land transitioned to Natural Vegetation, generating substantial ESV gains due to higher ecosystem service coefficients.

Table 11
Transition matrix of LULC Transitions and Ecosystem Service Values (Million USD/ha/yr) between 2000 and 2022.

LULC 2000\ LULC 2022	Water	Built-Up	Cultivated	Bare Land	Rock Land	Natural Vegetation	Total
Water	2.39	0.00	0.00	0.00	0.00	0.07	2.46
Built-Up Areas	0.00	5.59	0.32	0.00	0.00	0.02	5.93
Cultivated Areas	0.19	20.31	10.00	0.00	0.00	2.50	33.00
Bare Land	0.54	45.37	35.67	0.00	0.00	1.16	82.73
Rock Land	1.59	22.57	3.53	0.00	0.00	116.83	144.52
Natural Vegetation	0.53	0.55	0.77	0.00	0.00	75.18	77.03

3.7. Spatial redistribution and degradation hotspots

Although total ESV increased, spatial analysis indicates growing inequality in ecosystem service provision. Gains in Natural Vegetation were largely concentrated in upland and less accessible areas, whereas losses were focused in lower wadi corridors and coastal plains zones with high socio-economic pressure (Fig. 9).

Urban expansion after 2011 emerged as the dominant driver of ESV redistribution (Fig. 9). Built-Up Areas gained economic value, but this increase primarily reflects infrastructural and socio-economic valuation rather than enhancement of regulating or supporting ecosystem services. Meanwhile, the contraction of Cultivated Areas implies reductions in provisioning services such as food production and soil fertility regulation. Degradation hotspots are concentrated in middle wadi reaches and coastal zones, where urban growth overlaps with agricultural decline and vegetation fragmentation. These areas exhibit increased vulnerability to erosion, flooding, and habitat loss. Wadi Jazan has transitioned from agriculture-driven expansion (2000–2011) to urban-dominated transformation (2011–2022). While total ESV increased numerically, spatial redistribution and class-specific losses reveal localized ecosystem service degradation and growing inequality.

4. Discussion

This study demonstrates that land use and land cover (LULC) dynamics in Wadi Jazan from 2000 to 2022 are shaped by coupled environmental constraints and rapid socio-economic transformation. By integrating LULC transitions with ecosystem service valuation (ESV), the findings reveal not only landscape reconfiguration but also structural shifts in ecosystem service provision. The discussion situates these results within regional and global dryland research, while critically examining trade-offs, spatial inequalities, and methodological implications. Specific land-use transitions have direct implications for ecosystem services. The conversion of cultivated land to built-up areas reduces provisioning services such as food production while diminishing regulating services including soil fertility and water infiltration. Similarly, the loss of natural vegetation weakens flood regulation, carbon sequestration, and biodiversity support. Although vegetation expansion in upland areas contributes positively to regulating services, these gains do not compensate for losses in highly productive lowland zones.

4.1. Coupled controls of topography, climate, and human activity

The pronounced west–east elevation gradient fundamentally structures land use patterns in Wadi Jazan. Fertile alluvial soils and higher water availability in coastal plains and wadi floodplains favor agriculture and urban development, whereas upland and mountainous areas remain dominated by bare and rocky land due to shallow soils, reduced moisture retention, and limited accessibility. Similar topographically constrained land use patterns have been documented in arid and semi-arid watersheds worldwide [41, 42]. Climatic seasonality reinforces these gradients. Concentrated late-summer rainfall enhances short-term vegetation growth and agricultural productivity, particularly in downstream zones, but simultaneously increases flood risk. Seasonal hydrological pulses help explain the clustering of land transformation and ecosystem service

degradation in lower wadi sections, where development pressure and ecological vulnerability converge. Comparable interactions between hydrology, land conversion, and ecosystem risk have been reported in arid wadi systems in Oman, where upstream vegetation loss increased downstream flood hazards by 40–60% (91,92). Thus, LULC changes in Wadi Jazan are not solely development-driven; they are mediated by environmental constraints, including soil fertility, water availability, and flood-prone topography, creating spatially heterogeneous exposure to both opportunity and risk.

4.2. Agricultural expansion, decline, and urban acceleration

The period 2000–2011 reflects agricultural expansion consistent with broader dryland reclamation trends. Similar land conversion patterns were observed in Egypt's Nile Delta (+ 14.5%) [56] and Morocco's Souss Valley (≈ 30,000 ha converted) [57], reflecting food-security policies and irrigation development [32]. In Wadi Jazan, cultivated land expanded into previously uncultivated areas, reinforcing the importance of fertile wadi corridors [5, 53]. However, the subsequent contraction of cultivated land (2011–2022) represents a marked shift, resembling agricultural abandonment observed in China's Loess Plateau, where 23.4% of arable land was repurposed between 2000 and 2015, and aligning partially with regional transformations in Saudi Arabia, including Wadi Jazan and Al-Ahsa [58, 59]. This decline likely reflects urban encroachment, changing water availability, or shifting economic priorities.

Urbanization in Wadi Jazan has been particularly rapid. The ninefold increase in built-up area exceeds growth rates reported for Jeddah (3.2-fold) [60] and Riyadh (≈ 4-fold) [61], and parallels accelerated expansion in Al Baha after 2010 [62]. Comparable coastal urban growth has been documented in Bangladesh (6.8% annually) and other emerging coastal regions [1, 14]. Unlike desert cities such as Phoenix, where expansion often occupies marginal desert land [63], urban growth in Wadi Jazan largely encroached upon productive agricultural zones, intensifying socio-ecological trade-offs.

4.3. Vegetation restoration and landscape transformation

One notable outcome is the net increase in natural vegetation cover, contrasting with degradation trends reported in southwestern Saudi Arabia (1.2% annual decline) [64]. While improved detection from Landsat 8 may partly explain this pattern [65], ecological restoration and land abandonment likely contributed. Similar vegetation recovery has been documented in Mediterranean drylands and protected areas, as well as within Wadi Jazan. The conversion of rocky terrain to natural vegetation (≈ 29,207 ha) suggests partial regeneration in formerly degraded zones, potentially supported by improved water management or reduced grazing pressure. However, gains were spatially uneven, often concentrated in upland or less accessible areas, while ecologically sensitive lowland zones experienced fragmentation.

4.4. Trade-offs between provisioning, regulating, and urban services

The results reveal clear trade-offs between provisioning, regulating, and urban-associated services. Agricultural expansion enhanced provisioning services (food production) but reduced regulating and supporting functions through vegetation loss, soil modification, and increased water demand [1, 8, 13]. Urban expansion amplified these effects by replacing multifunctional ecosystems with impervious surfaces, reducing carbon sequestration, flood regulation, soil stabilization, and biodiversity maintenance [2, 36, 38]. Similar ecosystem service declines linked to urban growth have been reported in coastal Bangladesh and the Pearl River Delta [1, 26]. In semi-arid systems, short-term economic gains frequently compromise long-term ecological resilience, increasing vulnerability to erosion, water scarcity, and climate hazards [8, 13, 14]. Water bodies consistently displayed the highest per-unit ESV, highlighting their hydrological and regulatory importance [7, 9], yet their limited spatial extent constrains their capacity to offset widespread terrestrial losses.

4.5. Spatial inequality and coastal–fluvial vulnerability

ESV distribution in Wadi Jazan is highly heterogeneous. Degradation hotspots are concentrated in low-elevation coastal plains and downstream wadi sections, where urbanization, agricultural contraction, and population density converge. Similar hotspot patterns have been observed in coastal–fluvial systems elsewhere [8, 26]. In contrast, upland and mountainous areas function as ecological refugia due to limited accessibility [41, 42], though they remain vulnerable to future development and climate pressures. As an integrated coastal–fluvial system, Wadi Jazan faces distinct challenges, where

upstream land-use change can propagate downstream impacts across ecological boundaries. Comparable coastal systems in Mexico's Gulf of California experienced a 28% decline in mangrove ESV due to development [66], highlighting the importance of watershed-scale management in arid environments. The hydrological connection present in river systems generates distinct susceptibilities to alterations in upstream land use. Research on analogous wadi systems in Oman has shown that vegetation depletion in higher catchments can elevate flash flood hazards downstream by 40–60% [67, 68]. The recording of plant alterations in the higher reaches of Wadi Jazan has obvious implications for flood risk management in coastal urban areas.

4.6. Methodological reflections and research directions

The observed increase in total ESV despite fragmentation underscores methodological complexities, as aggregate ESV metrics can obscure ecological trade-offs [69]. The relatively high ESV coefficients assigned to urban areas reflect aggregated economic and cultural services rather than ecological functions, which may lead to overestimation of ecosystem service gains in urban contexts. Consequently, the increase in total ESV should be interpreted as a redistribution of service values across land-use types rather than an improvement in ecological condition, partly explaining divergence from studies using locally calibrated coefficients, such as in Ethiopia (37.4% ESV decline) and rapidly urbanizing Chinese regions reporting net ESV reductions [70]. This pattern aligns with global urbanization meta-analyses [71], where cultural and economic services increasingly dominate at the expense of regulating and provisioning functions.

The selection of 2000, 2011, and 2022 reflects the availability of high-quality Landsat imagery and captures long-term decadal change; however, discrete time points may overlook short-term dynamics. The use of six generalized LULC classes simplifies landscape heterogeneity and may mask ecological variability, particularly within vegetation and urban categories, though it ensures consistency with Landsat resolution and previous studies. Future research using higher-resolution and higher-frequency datasets could refine land-cover classification and improve detection of transitional dynamics.

Sensitivity analysis indicates that total ESV estimates are moderately affected by coefficient variation, particularly for high-value classes such as water bodies and built-up areas. Nevertheless, overall temporal trends and spatial patterns remain consistent, supporting the robustness of the study's conclusions despite uncertainty in coefficient selection. Classification errors, especially for built-up areas in earlier years, may propagate into ESV estimates due to the area-based calculation method. Misclassification between bare land, rock land, and built-up areas is a known limitation in semi-arid environments and may influence the magnitude of estimated ecosystem service values.

Wadi Jazan has transitioned from agriculture-driven expansion (2000–2011) to urban-dominated transformation (2011–2022). Although total ESV increased numerically, this reflects structural redistribution rather than uniform ecological improvement. The concentration of degradation in socio-economically critical coastal–fluvial zones highlights growing spatial inequality in ecosystem service provision. Balancing development with ecological sustainability in semi-arid coastal watersheds will require spatially targeted planning, upstream–downstream coordination, restoration of degraded corridors, and improved water governance. Without proactive management, continued urban acceleration may further erode regulating and supporting services that underpin long-term regional resilience.

Several limitations warrant attention. Reliance on global valuation coefficients may not fully capture local socio-ecological conditions; future work should develop region-specific coefficients using benefit transfer or locally calibrated approaches [72]. Additionally, broad LULC classes may obscure important ecological distinctions, and the absence of explicit socio-economic driver analysis limits causal interpretation. Integrating governance, demographic, and market data would strengthen future assessments.

4.7. Implications for sustainable land and ecosystem management

The land-use trajectory in Wadi Jazan reflects a transition from agriculture-driven expansion to rapid urban transformation, accompanied by increasing spatial concentration of ecosystem service degradation in coastal–fluvial zones. These patterns highlight the need to move beyond aggregate ecosystem service assessments toward spatially explicit, policy-relevant

planning frameworks. Effective management in semi-arid coastal watersheds requires targeted, ecosystem-based land-use planning that explicitly accounts for trade-offs among provisioning, regulating, and cultural services. Priority should be given to protecting high-value and vulnerable ecosystems, particularly remaining natural vegetation and water bodies in downstream and coastal areas where ecological functions and human pressures intersect. Establishing urban growth boundaries, promoting compact city development, and restricting expansion into fertile agricultural lands can help reduce further loss of critical ecosystem services.

Given the strong upstream–downstream linkages identified in the study, watershed-scale governance is essential. Coordinated management across elevation gradients can mitigate the propagation of land-use impacts, such as increased flood risk and reduced water regulation capacity. Restoration of degraded ecological corridors, especially along wadis and transitional zones, can enhance connectivity, improve hydrological regulation, and support biodiversity.

Sustainable agricultural practices should also be promoted to maintain provisioning services while minimizing pressure on soil and water resources. Integrating ecosystem service valuation into environmental impact assessments and land-use decision-making can support more balanced development strategies. Ecosystem-based management offers a practical pathway to reconcile rapid urbanization with ecological sustainability. Proactive, spatially differentiated interventions are critical to maintaining ecosystem functionality, reducing vulnerability to climate and hydrological risks, and ensuring long-term resilience in Wadi Jazan.

6. Conclusions

This study analyzed land use and land cover (LULC) dynamics and associated ecosystem service values (ESV) in Wadi Jazan, Saudi Arabia, from 2000 to 2022, providing insights into the interactions between environmental constraints, socio-economic development, and ecosystem functionality in a semi-arid coastal–fluvial system. The results reveal two distinct phases of landscape transformation: agricultural expansion (2000–2011) followed by rapid urbanization (2011–2022), with substantial conversion of agricultural and barren lands into built-up areas, particularly in coastal plains and mid-wadi corridors. Despite an overall increase in total ESV, this change primarily reflects a redistribution of ecosystem service values rather than a uniform improvement in ecological condition. Gains associated with urban and vegetation expansion were offset by declines in regulating and supporting services in key productive areas. Spatial analysis further revealed pronounced inequality in ecosystem service distribution, with degradation concentrated in socio-economically critical coastal–fluvial zones that are increasingly vulnerable to environmental risks. The findings highlight clear trade-offs between short-term development gains and long-term ecological sustainability. While urban expansion enhances economic and cultural services, it simultaneously reduces essential regulating functions such as flood mitigation, groundwater recharge, and climate regulation. These dynamics underscore the importance of incorporating spatial heterogeneity and ecosystem service trade-offs into land-use planning and policy frameworks. From a broader perspective, this study demonstrates that increases in aggregate ESV can mask underlying ecological degradation, particularly in rapidly transforming semi-arid environments. Sustainable development in such systems requires integrated, spatially explicit approaches that balance economic growth with the protection and restoration of critical ecosystem functions. The methodological framework applied in this study provides a replicable approach for monitoring LULC change and ecosystem service dynamics, offering a valuable tool for supporting evidence-based planning and sustainable land management in Wadi Jazan and comparable dryland coastal regions.

Declarations

Conflicts of Interest:

The authors declare no competing interests.

Funding:

This research was funded by the Deanship of Graduate Studies and Scientific Research, Taif University.

Author Contribution

Author Contributions: Conceptualization, I.A.H.Y., F.M.G.; M.M.M.; and M.A.A.; methodology, I.A.H.Y., and M.A.A.; software, M.A.A.; validation, I.A.H.Y., A.A.S.A., and M.A.A.; formal analysis, I.A.H.Y., W.A.O., A.F.A., and M.A.A.; investigation, I.A.H.Y., A.A.S.A., W.A.O., A.F.A., and M.A.A.; resources, I.A.H.Y., W.A.O., A.F.A., and A.A.S.A.; F.M.G.; M.M.M.; data curation, I.A.H.Y. and M.A.A.; writing—original draft preparation, I.A.H.Y., and M.A.A.; writing—review and editing, I.A.H.Y., A.E.I., and A.A.S.A.; visualization, I.A.H.Y., A.E.I., and M.A.A.; supervision, I.A.H.Y., A.E.I., and M.A.A.; project administration, I.A.H.Y. F.M.G.; M.M.M.; and M.A.A.; funding acquisition, I.A.H.Y., A.A.S.A. and M.A.A. All authors have read and agreed to the published version of the manuscript.

Acknowledgements:

The author would like to acknowledge Deanship of Graduate Studies and Scientific Research, Taif University for funding this work.

Data Availability

Data will be made available on request.

References

1. Hu, M. et al. Spatio-temporal changes in ecosystem service value in response to land-use/cover changes in the Pearl River Delta. *Resour. Conserv. Recycl.* **149**, 106–114 (2019).
2. Liu, W. et al. Spatio-temporal variations of ecosystem services and their drivers in the Pearl River Delta, China. *J. Clean. Prod.* **337**, 130466. https://doi.org/10.1016/j.jclepro.2022.130466 (2022).
3. Assessment, M. E. *Ecosystems and human well-being: wetlands and water*; World resources institute: (2005).
4. Mahmoud, S. H. & Gan, T. Y. Impact of anthropogenic climate change and human activities on environment and ecosystem services in arid regions. *Sci. Total Environ.* **633**, 1329–1344. 10.1016/j.scitotenv.2018.03.290 (2018).
5. Shang, Y., Wang, D., Liu, S. & Li, H. Spatial-Temporal Variation and Mechanisms Causing Spatial Differentiation of Ecosystem Services in Ecologically Fragile Regions Based on Value Evaluation: A Case Study of Western Jilin, China. *Land* **11**, 629. https://doi.org/10.3390/land11050629 (2022).
6. Yousif, I. A. et al. Spatial analysis of desertification-sensitive areas in arid conditions based on modified MEDALUS approach and geospatial techniques. *Open. Agric.* **10**, 20250453. https://doi.org/10.1515/opag-2025-0453 (2025).
7. Yan, F. et al. The effects of spatiotemporal changes in land degradation on ecosystem services values in Sanjiang Plain, China. *Remote Sens.* **8**, 917. https://doi.org/10.3390/rs8110917 (2016).
8. Ren, B. et al. Assessment of ecosystem services: spatio-temporal analysis and the spatial response of influencing factors in hainan province. *Sustainability* **14**, 9145. https://doi.org/10.3390/su14159145 (2022).
9. Sun, Y. et al. Spatio-temporal evolution scenarios and the coupling analysis of ecosystem services with land use change in China. *Sci. Total Environ.* **681**, 211–225 (2019).
10. Selmy, S. A. et al. Land Suitability Assessment and Crop Water Requirements for Twenty Selected Crops in an Arid Land Environment. *Agronomy* **14**, 2601. https://doi.org/10.3390/agronomy14112601 (2024).

11. Yousif, I. A. H. Optimizing Agricultural Land Evaluation of Some Areas in the New Delta Region, Al–Dabaa Corridor, Egypt. *Egypt. J. Soil Sci.* **64**, 193–206. 10.21608/EJSS.2023.239906.1669 (2024).
12. Schirpke, U., Tscholl, S. & Tasser, E. Spatio-temporal changes in ecosystem service values: Effects of land-use changes from past to future (1860–2100). *J. Environ. Manage.* **272**, 111068. 10.1016/j.jenvman.2020.111068 (2020).
13. Gao, F. et al. Spatio-Temporal distribution and driving factors of ecosystem service value in a fragile hilly area of North China. *Land* **11**, 2242. https://doi.org/10.3390/land11122242 (2022).
14. Cheng, Y. et al. Impact of urbanization on ecosystem service value from the perspective of spatio-temporal heterogeneity: a case study from the Yellow River Basin. *Land* **12**, 1301. https://doi.org/10.3390/land12071301 (2023).
15. Ahmed, A. S., Yousif, I. A. H. & Atalla, M. A. Land Degradation and Deforestation Monitoring and Assessment of West Africa Lands for Sustainable Agricultural Development Using Moderate Resolution Imaging Spectroradiometer (MODIS) Imagery Processing Techniques. In Microclimate Monitoring, Mitigation and Adaptation in Deltas, (eds Nasr, M. & Negm, A.) Springer Nature Switzerland: Cham, ; 83–115. (2026).
16. Song, J. et al. Spatio-Temporal fluctuation analysis of ecosystem service values in Northeast China over long time series: based on bayesian hierarchical modeling. *Land* **13**, 833. https://doi.org/10.3390/land13060833 (2024).
17. Yousif, I. A. et al. Soil quality indicator-based land productivity modelling for agricultural sustainability. *PloS one*. **20**, e0316840. 10.1371/journal.pone.0316840 (2025).
18. Shokr, M. S. et al. Assessment of soil quality in arid zones using principal component analysis and GIS-based modeling. *PLoS One*. **20**, e0337063. 10.1371/journal.pone.0337063 (2025).
19. Atalla, M. A., Alenezi, M. S., Ahmed, A. A. R. S. & Yousif, I. A. H. Comparative assessment of desertification sensitivity in West Africa using standard and FAHP-modified MEDALUS approach. *Ecol. Ind.* **183**, 114692. https://doi.org/10.1016/j.ecolind.2026.114692 (2026).
20. Garah, K. et al. Retrospective Study of the Impact of the 2021 Forest Fires on Land Areas in Algeria: The Case of Khenchela Forests. *Fire Mater.* https://doi.org/10.1002/fam.70038 (2026).
21. Altuwaijri, H. A., Al Kafy, A. & Rahaman, Z. A. Multi-temporal remote sensing and geospatial analysis for urban ecosystem service dynamics: A three-decade assessment of land surface transformation in Jeddah, Saudi Arabia. *Phys. Chem. Earth Parts A/B/C*. **139**, 103892. https://doi.org/10.1016/j.pce.2025.103892 (2025).
22. Bindajam, A. A., Mallick, J., Talukdar, S., Islam, A. R. M. T. & Alqadhi, S. Integration of artificial intelligence–based LULC mapping and prediction for estimating ecosystem services for urban sustainability: past to future perspective. *Arab. J. Geosci.* **14**, 1887. https://doi.org/10.1007/s12517-021-08251-4 (2021).
23. Souici, I. & Zouak, Z. Land Use/Land-Cover changes and their impacts on ecosystem services values: a spatio-temporal analysis in Mila, Algeria from 1994–2024. *Indonesian J. Social Sci. Res.* **5**, 471–483. http://dx.doi.org/10.11594/ijssr.05.02.09 (2024).
24. Yousif, I. A. H., Land Evaluation & Assessment of Land Cover Change Using Geospatial Techniques. A Case Study in West Samlout Area, Egypt. *Egypt. J. Soil Sci.* **64**, 485–506. https://doi.org/10.21608/ejss.2024.260713.1708 (2024).
25. Haddad, S. A. et al. Impact of Flooding on Lands with Emerging Contaminants on the Quality of Receiving Water Bodies. *Water* **16**, 3214. https://doi.org/10.3390/w16223214 (2024).
26. Hoque, M. Z., Islam, I., Ahmed, M., Hasan, S. S. & Prodhan, F. A. Spatio-temporal changes of land use land cover and ecosystem service values in coastal Bangladesh. *Egypt. J. Remote Sens. Space Sci.* **25**, 173–180 (2022).
27. Yousif, I. A. et al. Efficiency of Geostatistical Approach for Mapping and Modeling Soil Site-Specific Management Zones for Sustainable Agriculture Management in Drylands. *Agronomy* **14**, 2681. https://doi.org/10.3390/agronomy14112681 (2024).
28. Kafy, A. A. & Altuwaijri, H. A. Eco-climatological modeling approach for exploring spatiotemporal dynamics of ecosystem service values in response to land use and land cover changes in Riyadh, Saudi Arabia. *Theoret. Appl. Climatol.* **155**, 9497–9516. 10.1007/s00704-024-05199-9 (2024).

29. Getahun, A. B., Dagnew, A. B. & Ayal, D. Y. Spatio-temporal dynamics of ecosystem service value functions in response to landscape fragmentation in Boma-Gambella trans-boundary landscape, Southwest Ethiopia and East South Sudan: AB Getahun et al. *Discover Appl. Sci.* **7**, 804. https://doi.org/10.1007/s42452-025-07082-2 (2025).
30. Gillman, M. Primary results of a geological and geophysical reconnaissance of the Jizan coastal plain in Saudi Arabia. In Proceedings of the SPE Middle East Regional Meeting, ; pp. SPE-2370-MS. (1968).
31. Youssef, A. M., Pradhan, B., Sabtan, A. A. & El-Harbi, H. M. Coupling of remote sensing data aided with field investigations for geological hazards assessment in Jazan area, Kingdom of Saudi Arabia. *Environ. Earth Sci.* **65**, 119–130. https://doi.org/10.1007/s12665-011-1071-3 (2012).
32. Yousif, I., Tealab, E., Hady, A. & Aldabaa, A. Spatial soil erosion risk assessment using CORINE model: a case study in Wadi El-Raml Watershed, North Western Coast. *Egypt. Plant. Arch.* **20**, 705–714 (2020).
33. Hamed, M. A., Kasem, W. T. & Shalabi, L. F. Floristic diversity and vegetation-soil correlations in Wadi Qusai, Jazan, Saudi Arabia. *Int. J. Plant. Soil. Sci.* **25**, 1–18. 10.9734/IJPSS/2018/44508 (2018).
34. Khawfany, A. A., Aref, M. A., Matsah, M. I. & Taj, R. J. Utilizing Landsat-8 data in mapping of sabkha, mangroves, and land covers in Jizan coastal plain, southwestern Saudi Arabia. *Arab. J. Geosci.* **10**, 103. https://doi.org/10.1007/s12517-017-2904-5 (2017).
35. Valjarević, A. et al. The coastal fog and ecological balance for plants in the Jizan region, Saudi Arabia. *Saudi J. Biol. Sci.* **30**, 103494. 10.1016/j.sjbs.2022.103494 (2023).
36. Costanza, R. et al. The value of the world's ecosystem services and natural capital. *nature 387*, 253–260, (1997). https://doi.org/10.1038/387253a0
37. Costanza, R. et al. Changes in the global value of ecosystem services. *Glob. Environ. Change*. **26**, 152–158. https://doi.org/10.1016/j.gloenvcha.2014.04.002 (2014).
38. De Groot, R. et al. Global estimates of the value of ecosystems and their services in monetary units. *Ecosyst. Serv.* **1**, 50–61. https://doi.org/10.1016/j.ecoser.2012.07.005 (2012).
39. Al-Zubieri, A. G. et al. Application of GIS and remote sensing to monitor the impact of development activities on the coastal zone of Jazan City on the Red Sea, Saudi Arabia. *Int. Archives Photogrammetry Remote Sens. Spat. Inform. Sci.* **42**, 45–50. https://doi.org/10.5194/isprs-archives-XLII-3-W4-45-2018 (2018).
40. Wang, Y., Zhang, X. & Peng, P. Spatio-Temporal Changes of Land-Use/Land Cover Change and the Effects on Ecosystem Service Values in Derong County, China, from 1992–2018. *Sustainability* **13**, 827 (2021).
41. Khadka, N., Zhang, G. & Thakuri, S. Glacial lakes in the Nepal Himalaya: Inventory and decadal dynamics (1977–2017). *Remote Sens.* **10**, 1913. https://doi.org/10.3390/rs10121913 (2018).
42. Xie, G., Lu, C. X., Leng, Y. F. & Zheng, D. LI, S.-c. Ecological assets valuation of the Tibetan Plateau. *J. Nat. Resour.* **18**, 189–196 (2003).
43. Chavez, P. S. An improved dark-object subtraction technique for atmospheric scattering correction of multispectral data. *Remote Sens. Environ.* **24**, 459–479. https://doi.org/10.1016/0034-4257(88)90019-3 (1988).
44. Chen, C. et al. The application of the tasseled cap transformation and feature knowledge for the extraction of coastline information from remote sensing images. *Adv. Space Res.* **64**, 1780–1791. https://doi.org/10.1016/j.asr.2019.07.032 (2019).
45. Richards, J. A. & Jia, X. *Remote Sensing Digital Image Analysis* 4 edn (Springer, 2006).
46. Manandhar, R., Odeh, I. O. & Ancev, T. Improving the accuracy of land use and land cover classification of Landsat data using post-classification enhancement. *Remote Sens.* **1**, 330–344. https://doi.org/10.3390/rs1030330 (2009).
47. Rai, R., Zhang, Y., Paudel, B., Acharya, B. K. & Basnet, L. Land use and land cover dynamics and assessing the ecosystem service values in the trans-boundary Gandaki River Basin, Central Himalayas. *Sustainability 10*, 3052, (2018). https://doi.org/10.3390/su10093052

48. Sun, X., Crittenden, J. C., Li, F., Lu, Z. & Dou, X. Urban expansion simulation and the spatio-temporal changes of ecosystem services, a case study in Atlanta Metropolitan area, USA. *Sci. Total Environ.* **622**, 974–987. 10.1016/j.scitotenv.2017.12.062 (2018).
49. Wang, S. W., Gebru, B. M., Lamchin, M., Kayastha, R. B. & Lee, W. K. Land use and land cover change detection and prediction in the Kathmandu district of Nepal using remote sensing and GIS. *Sustainability* **12**, 3925. https://doi.org/10.3390/su12093925 (2020).
50. Liu, X. H., Skidmore, A. K. & Van Oosten, H. Integration of classification methods for improvement of land-cover map accuracy. *ISPRS J. Photogrammetry Remote Sens.* **56**, 257–268. https://doi.org/10.1016/S0924-2716(02)00061-8 (2002).
51. Richards, J. A. Supervised classification techniques. In *Remote sensing digital image analysis*; Springer: ; pp. 263–367. (2022).
52. Lin, T., Xue, X., Shi, L. & Gao, L. Urban spatial expansion and its impacts on island ecosystem services and landscape pattern: A case study of the island city of Xiamen, Southeast China. *Ocean. Coastal. Manage.* **81**, 90–96. https://doi.org/10.1016/j.ocecoaman.2012.06.014 (2013).
53. Shrestha, S., Poudyal, K. N., Bhattarai, N., Dangi, M. B. & Boland, J. J. An Assessment of the Impact of Land Use and Land Cover Change on the Degradation of Ecosystem Service Values in Kathmandu Valley Using Remote Sensing and GIS. *Sustainability* **14**, 15739. https://doi.org/10.3390/su142315739 (2022).
54. Kindu, M., Schneider, T., Teketay, D. & Knoke, T. Changes of ecosystem service values in response to land use/land cover dynamics in Munessa–Shashemene landscape of the Ethiopian highlands. *Sci. Total Environ.* **547**, 137–147. 10.1016/j.scitotenv.2015.12.127 (2016).
55. Tolessa, T., Senbeta, F. & Kidane, M. The impact of land use/land cover change on ecosystem services in the central highlands of Ethiopia. *Ecosyst. Serv.* **23**, 47–54. https://doi.org/10.1016/j.ecoser.2016.11.010 (2017).
56. El-Hamid, H. T. A., Nour-Eldin, H., Rebouh, N. Y. & El-Zeiny, A. M. Past and future changes of land use/land cover and the potential impact on ecosystem services value of Damietta Governorate, Egypt. *Land* **11**, 2169. https://doi.org/10.3390/land11122169 (2022).
57. Ardakani, M. A. H., Cheshmberah, F. & Mokhtari, M. H. Investigating the Effects of Land Use Changes on Trend of Desertification Using Remote Sensing (Case Study: Abarkooh Plain, Yazd, Iran). *Journal of Rangeland Science 7*. (2017).
58. Abd El-Hamid, H. T., Hafiz, M. A., Wenlong, W. & Qiaomin, L. Detection of Environmental Degradation in Jazan Region on the Red Sea, KSA, Using Mathematical Treatments of Remote Sensing Data. *Remote Sens. Earth Syst. Sci.* **2**, 183–196. https://doi.org/10.1007/s41976-019-00022-w (2019).
59. Hereher, M., Alghmdi, A., Mseddi, K. & El Kenawy, A. Remote sensing of vegetation prolonged drought at the salt playas of Hail–Saudi Arabia. *Egypt. J. Remote Sens. Space Sci.* **25**, 135–145. https://doi.org/10.1016/j.ejrs.2022.01.006 (2022).
60. Aljoufie, M., Zuidgeest, M., Brussel, M. & van Maarseveen, M. Spatial–temporal analysis of urban growth and transportation in Jeddah City, Saudi Arabia. *Cities* **31**, 57–68. https://doi.org/10.1016/j.cities.2012.04.008 (2013).
61. Alqadhi, S., Bindajam, A. A., Mallick, J., Shahfahad; Rahman, A. & Talukdar, S. Mapping and evaluating sustainable and unsustainable urban areas for ecological management towards achieving low-carbon city: an empirical study of Asir Region, Saudi Arabia. *Environ. Sci. Pollut. Res.* **30**, 65916–65932. https://doi.org/10.1007/s11356-023-27129-4 (2023).
62. Alsharif, M., Alzandi, A. A., Shrahily, R. & Mobarak, B. Land Use Land Cover Change Analysis for Urban Growth Prediction Using Landsat Satellite Data and Markov Chain Model for Al Baha Region Saudi Arabia. *Forests* **13**, 1530 (2022).
63. Buyantuyev, A. & Wu, J. Urbanization diversifies land surface phenology in arid environments: Interactions among vegetation, climatic variation, and land use pattern in the Phoenix metropolitan region, USA. *Landsc. Urban Plann.* **105**, 149–159. https://doi.org/10.1016/j.landurbplan.2011.12.013 (2012).
64. El-Rawy, M. et al. Climate change impacts on water resources in arid and semi-arid regions: a case study in Saudi Arabia. *Water* **15**, 606. https://doi.org/10.3390/w15030606 (2023).

65. López-Serrano, P. M., Corral-Rivas, J. J., Díaz-Varela, R. A., Álvarez-González, J. G. & López-Sánchez, C. A. Evaluation of radiometric and atmospheric correction algorithms for aboveground forest biomass estimation using Landsat 5 TM data. *Remote Sens.* **8**, 369. https://doi.org/10.3390/rs8050369 (2016).
66. Antúnez, P. Mangrove Area Trends in Mexico Due to Anthropogenic Activities: A Synthesis of Five Decades (1970–2020). *Coasts* **4**, 726–739. https://doi.org/10.3390/coasts4040038 (2024).
67. Abdalla, F., Al-Turki, A. & Al Amri, A. Evaluation of groundwater resources in the Southern Tihama plain, Saudi Arabia. *Arab. J. Geosci.* **8**, 3299–3310. https://doi.org/10.1007/s12517-014-1401-3 (2015).
68. Yousif, I. A., Hady, A. A. A. & Aldabaa, A. A. Hydropedological Assessment of Wadi El-Raml at the Northwestern Coast of Egypt. *Sci. Afr.* **17**, e01322. https://doi.org/10.1016/j.sciaf.2022.e01322 (2022).
69. Schröter, M. et al. Ecosystem services as a contested concept: a synthesis of critique and counter-arguments. *Conserv. Lett.* **7**, 514–523. https://doi.org/10.1111/conl.12091 (2014).
70. Su, S., Xiao, R., Jiang, Z. & Zhang, Y. Characterizing landscape pattern and ecosystem service value changes for urbanization impacts at an eco-regional scale. *Appl. Geogr.* **34**, 295–305. https://doi.org/10.1016/j.apgeog.2011.12.001 (2012).
71. Luo, F., He, L., He, Z., Zeng, W. & Wang, Y. Evaluation of Coastal Ecological Security Barrier Functions Based on Ecosystem Services: A Case Study of Fujian Province, China. *Sustainability* **16**, 6787. https://doi.org/10.3390/su16166787 (2024).
72. Robert, J., John, J. & Ewa, R. Benefit transfer of environmental and resource values: progress, prospects and challenges. *Benefit Transf. Environ. Resource Values: Progress Prospects Challenges*. **12**, 177–266. https://doi.org/10.1561/101.00000102 (2018).

Figures

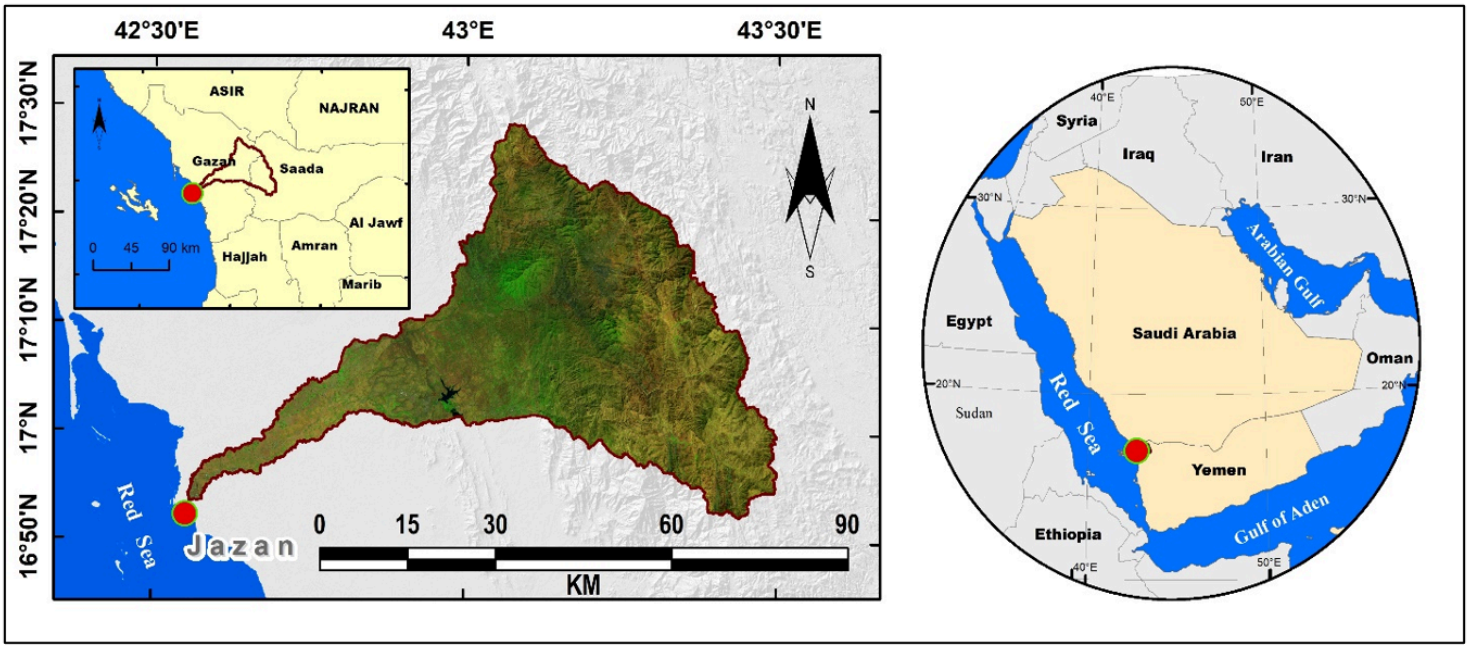


Figure 1

Map showing the location and spatial extent of the Jazan study area in southwestern Saudi Arabia along the eastern Red Sea coast (16°50'–17°30' N, 42°30'– 43°30' E), produced using ArcGIS Pro 3.4.

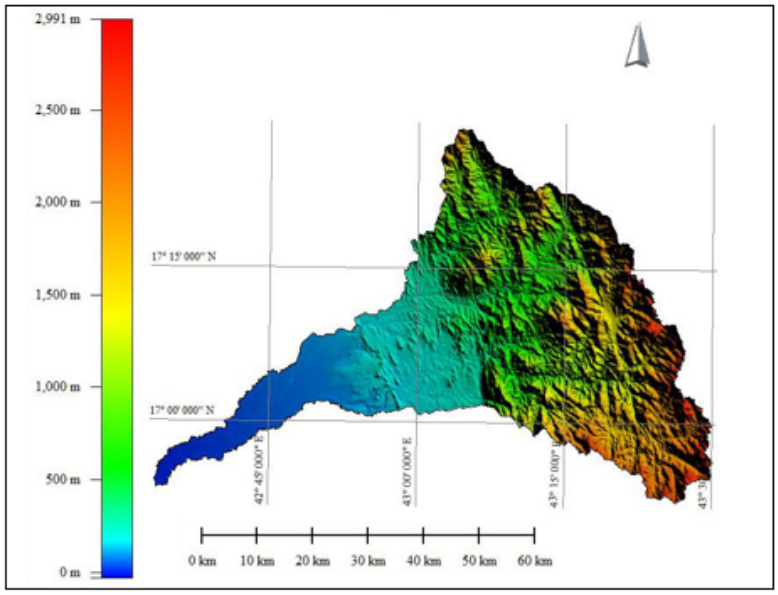


Figure 2

Digital Elevation Model (DEM) illustrating the topographic characteristics and elevation gradients of the Jazan study area.

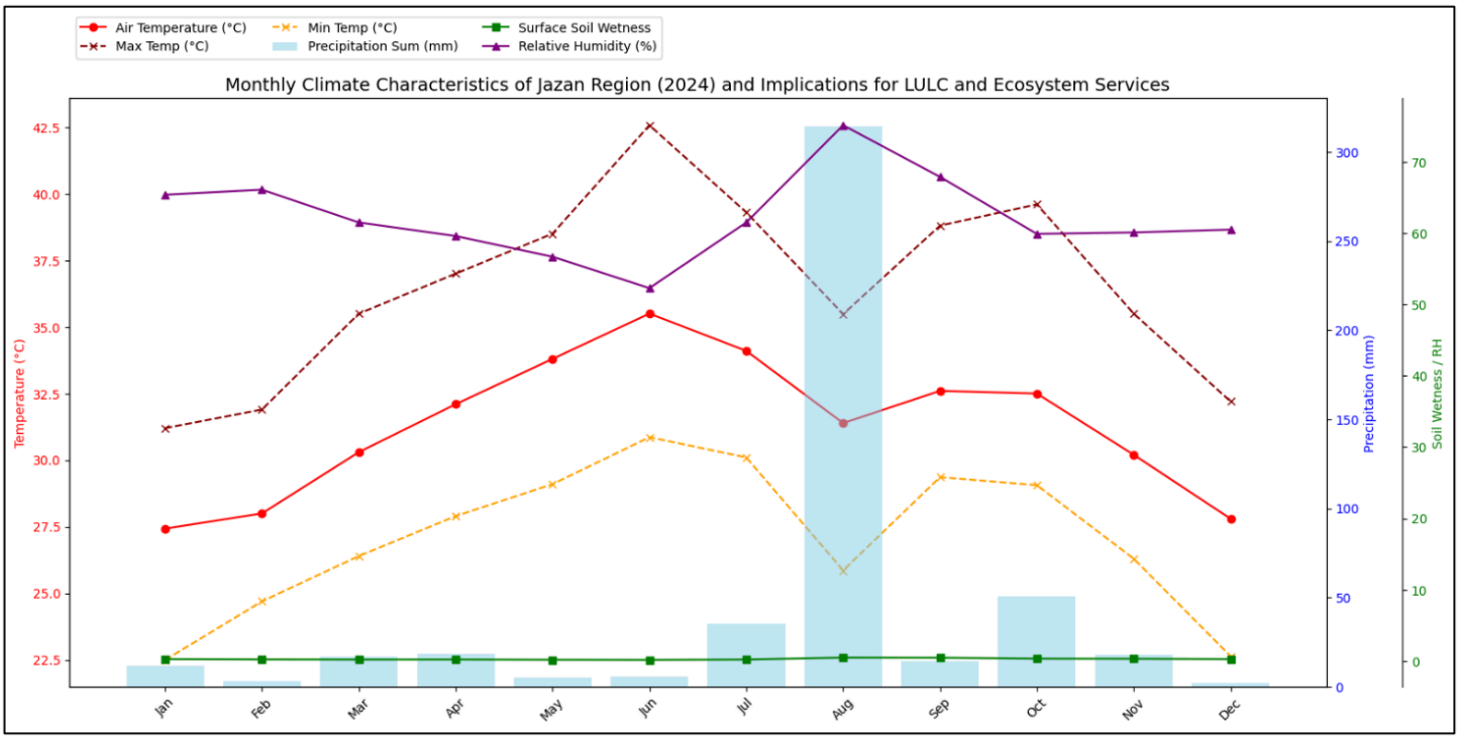


Figure 3

Monthly climatic variability of the Jazan region in 2024 and its implications for land use/land cover (LULC) patterns and ecosystem service dynamics.

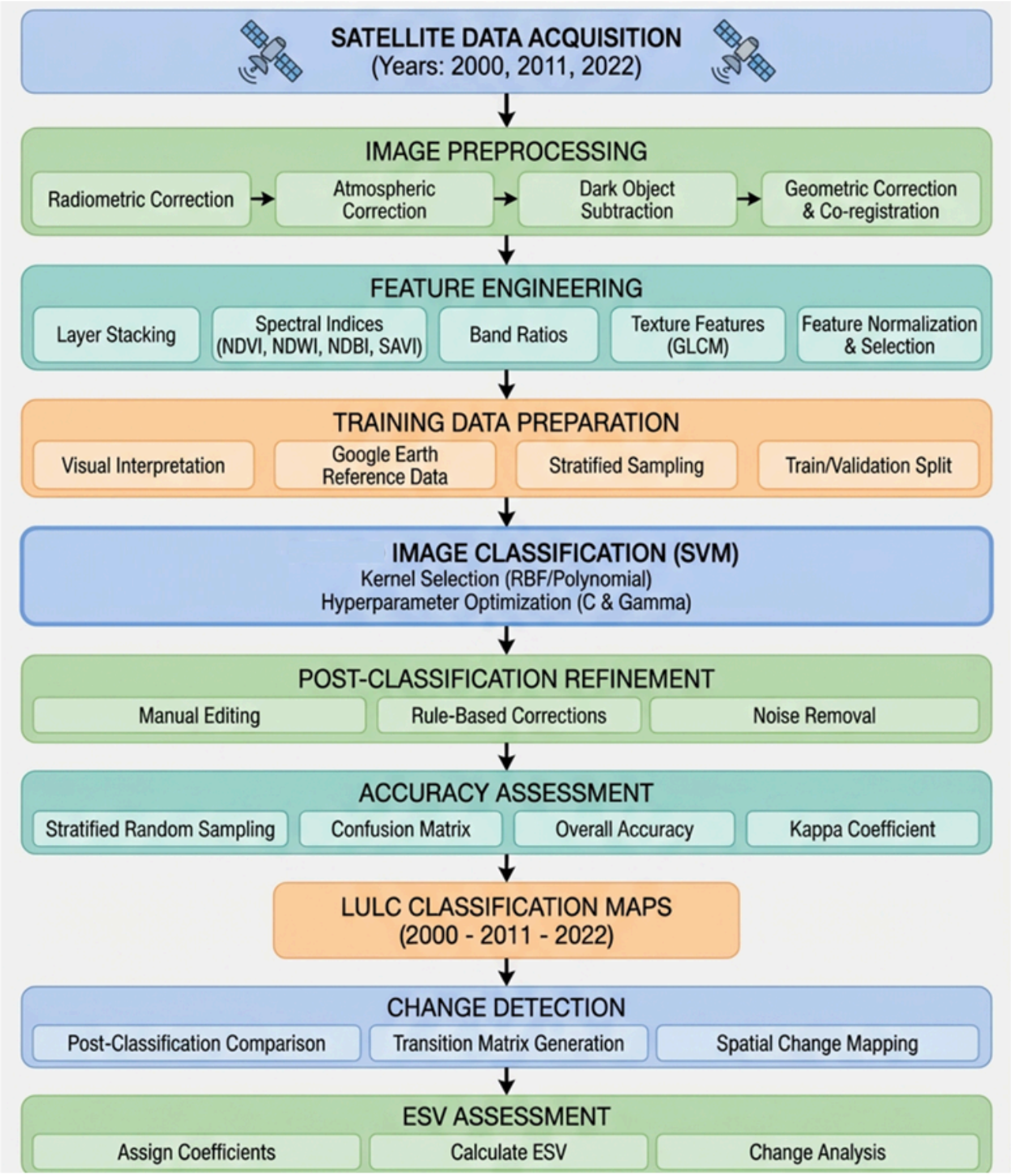


Figure 4

Conceptual workflow illustrating the methodological framework adopted for data preprocessing, land use/land cover classification, change detection, and ecosystem service value assessment.

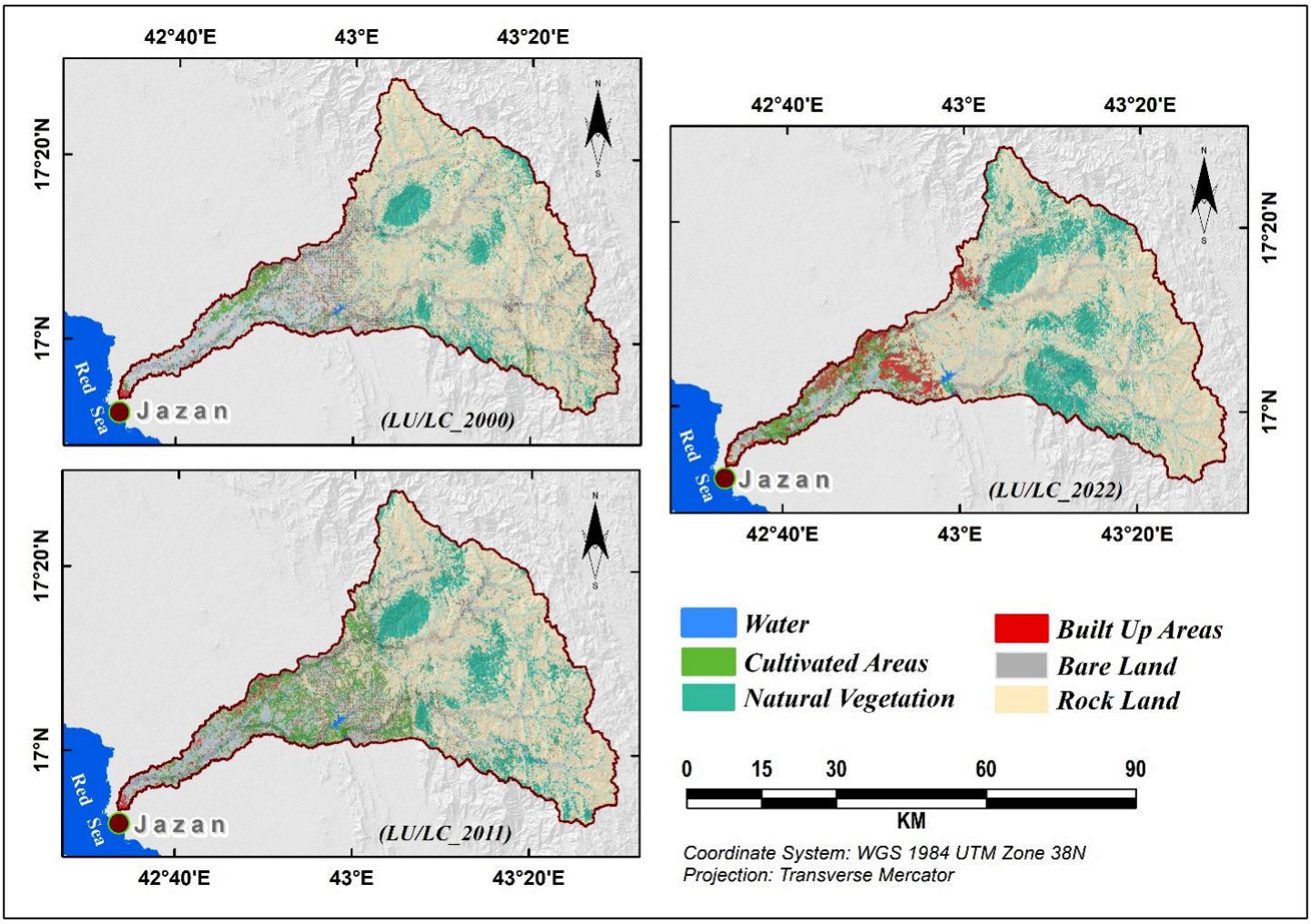


Figure 5

Spatial Distribution of LULC in Jazan Valley for 2000, 2011, and 2022 Based on Supervised Classification of Landsat Imagery.

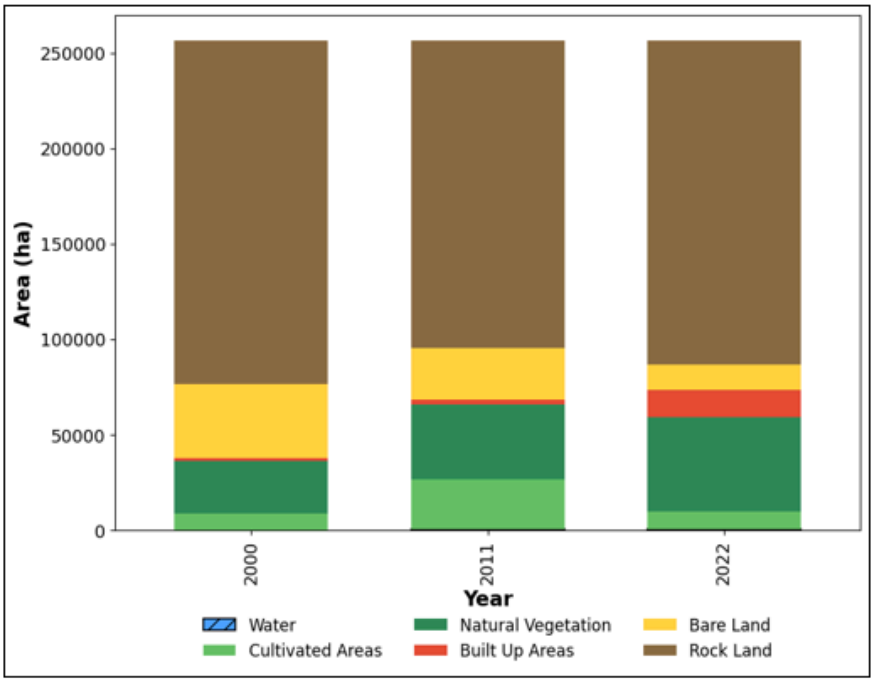


Figure 6

Temporal dynamics of land cover categories (hectares) in the Jazan Valley for 2000, 2011, and 2022.

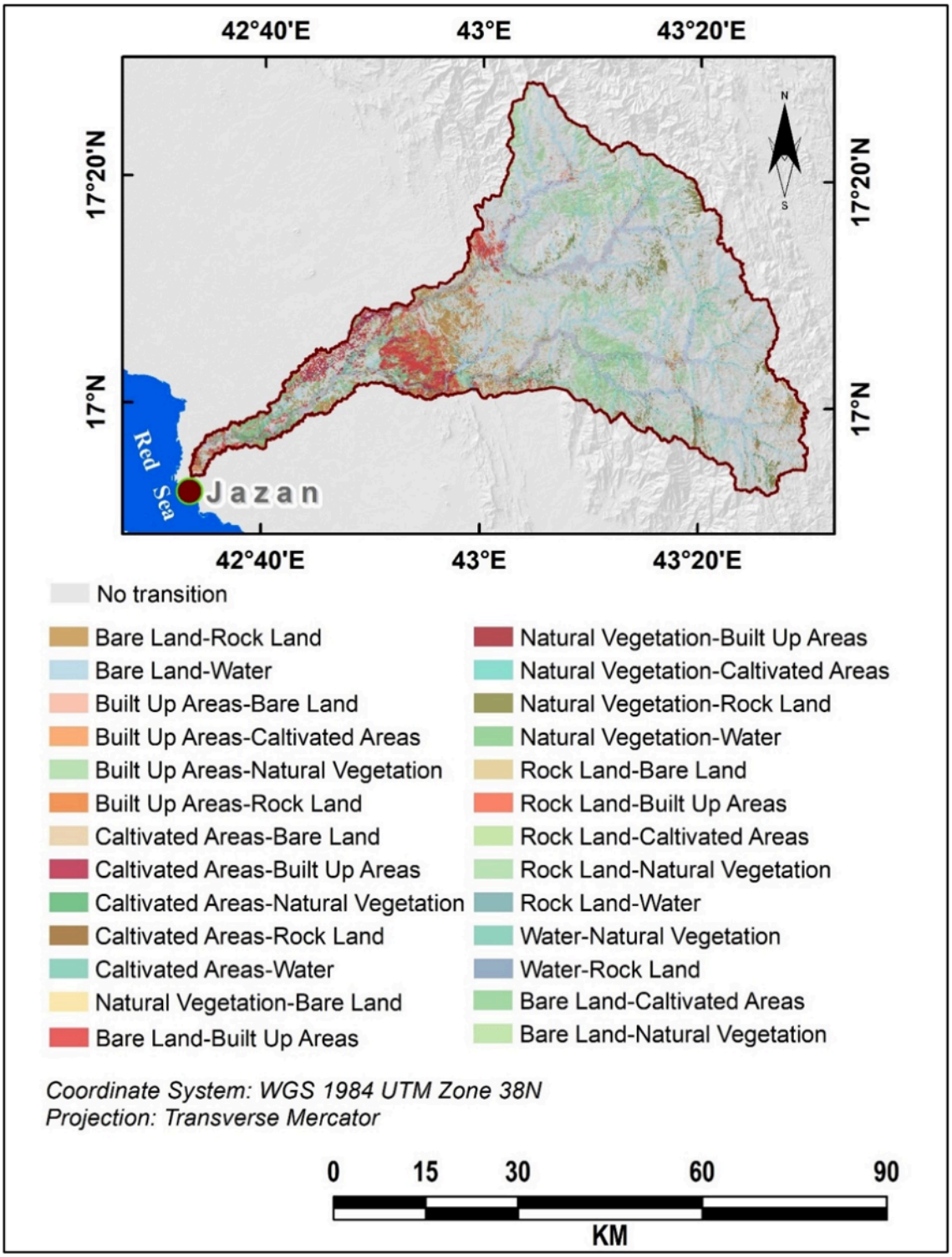


Figure 7

Spatial distributionof land use/land cover (LULC) class transitions in the Jazan Valley from 2000 to 2022.

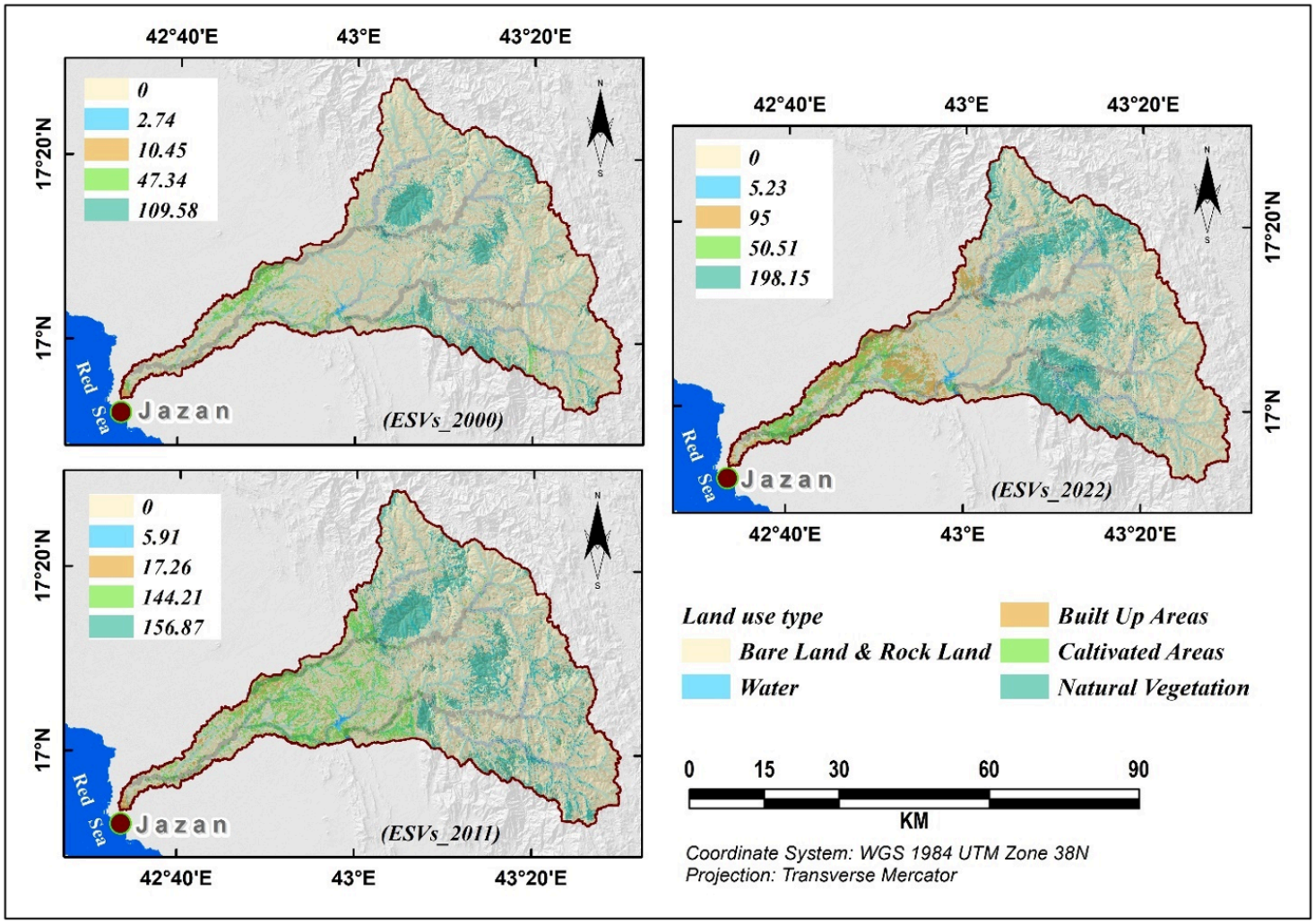


Figure 8

Distribution of ecosystem service values among LULC classes during the study period (2000–2022).

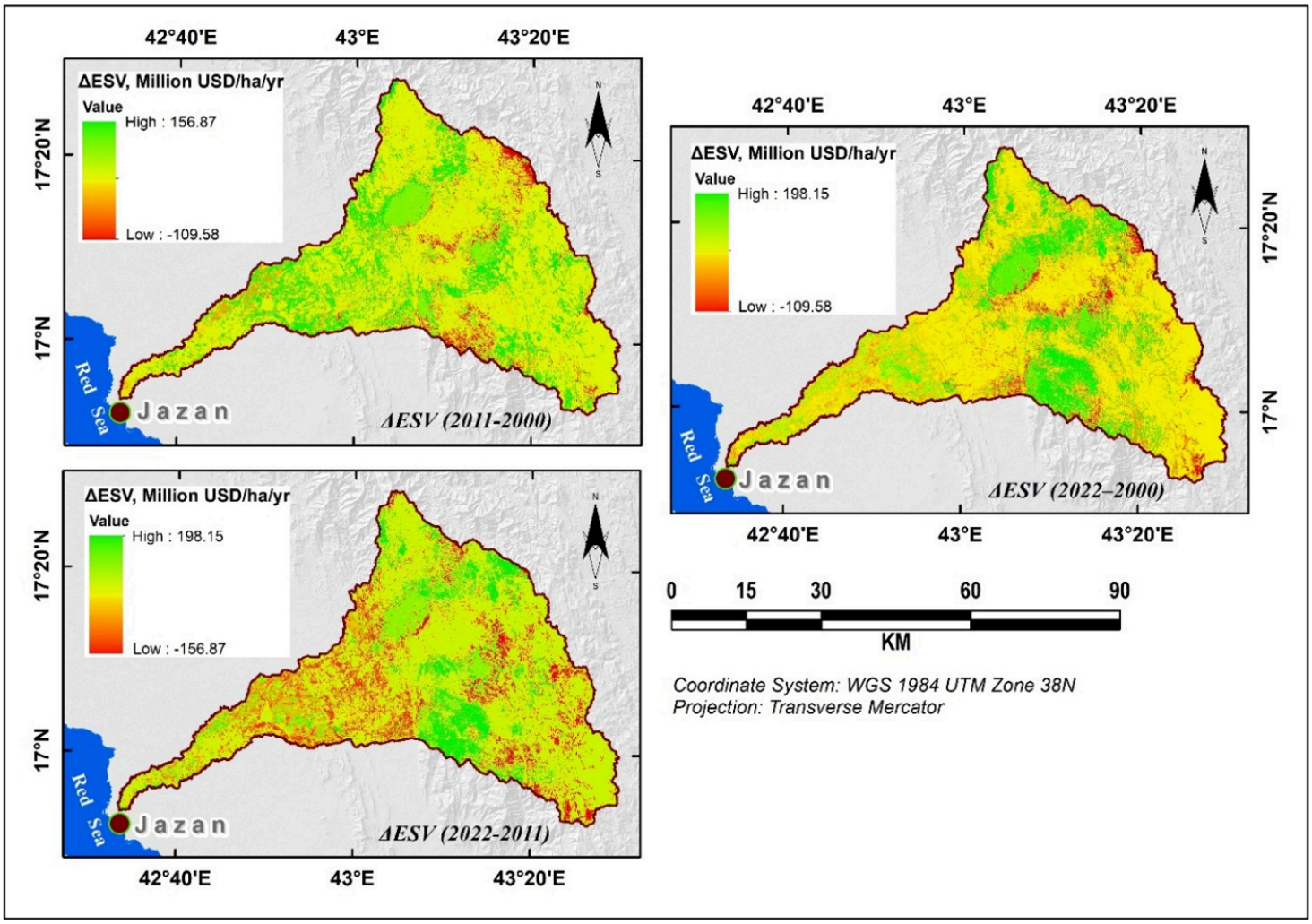


Figure 9

Spatial distribution of ecosystem service values (ESV) in Wadi Jazan (2000–2022).